UNIVERSITY OF CALIFORNIA SAN DIEGO

Centrifugal Cleansing of the Subchondral Bone of Osteochondral Grafts

A dissertation submitted in partial satisfaction of the

requirements for the degree Doctor of Philosophy

in

Bioengineering

by

Rebecca L Drake

Committee in Charge:

Professor Robert L Sah, Chair
Professor Francisco J Contijoch
Professor Monica Guma
Professor Koichi Masuda
Professor Lingyan Shi

2022

The Dissertation of Rebecca L Drake is approved, and it is acceptable in quality and form for publication on microfilm and electronically.

University of California San Diego

2022

EPIGRAPH

O Captain! my Captain! our fearful trip is done,
The ship has weather'd every rack, the prize we sought is won,
The port is near, the bells I hear, the people all exulting,
While follow eyes the steady keel, the vessel grim and daring;
But O heart! heart! heart!
O the bleeding drops of red,
Where on the deck my Captain lies,
Fallen cold and dead.

O Captain! my Captain! rise up and hear the bells;
Rise up—for you the flag is flung—for you the bugle trills,
For you bouquets and ribbon'd wreaths—for you the shores a-crowding,
For you they call, the swaying mass, their eager faces turning;
Here Captain! dear father!
This arm beneath your head!
It is some dream that on the deck,
You've fallen cold and dead.

My Captain does not answer, his lips are pale and still,
My father does not feel my arm, he has no pulse nor will,
The ship is anchor'd safe and sound, its voyage closed and done,
From fearful trip the victor ship comes in with object won;
Exult O shores, and ring O bells!
But I with mournful tread,
Walk the deck my Captain lies,
Fallen cold and dead.

Walt Witman
O Captain! My Captain!

TABLE OF CONTENTS

LIST OF FIGURES

LIST OF TABLES

ACKNOWLEDGEMENTS

I would first like to acknowledge my graduate research advisor and committee chair, Dr. Robert Sah. Thank you for the opportunity to learn from your expertise. I want to thank you for the countless hours spent working on projects, proposals, and papers especially regarding troubleshooting experiments and presenting data efficiently. I am truly grateful for the growth I have experienced over the past years and will think of my time in the Cartilage Tissue Engineering lab fondly.

I would also like to thank the other members of my dissertation committee: Profs. Francisco Contijoch, Monica Guma, Koichi Masuda, and Lingyan Shi for their valuable input and feedback on this project. Thank you for your insightful questions and suggestions that helped shape this dissertation.

I would like to thank the members (both current and former) of the CTE lab who have helped me in every aspect over the years. Albert, thank you for teaching me so many valuable skills in the lab and thank you also for teaching me the various soft skills that come with being a researcher in the CTE lab. Van, thank you for your help troubleshooting and also for keeping cool and collected when research gets stressful. Erica, you have been with me since day 1 (day 0 if you count the interview for the program), I have enjoyed spending long days and late nights troubleshooting, harvesting, and generally leaning on you for support. Ismael, Nasim, and Alborz, I have enjoyed working alongside you for the last few years and I thank you also for helping and supporting me, especially in the final stages of my thesis.

Finally, I am grateful for the support of my family and friends during my time at UCSD. I have been so lucky to have such a great PhD cohort, you have been so supportive and fun since the beginning of this program. I thank you all for letting me lean on you through all the trials of the PhD. I have also been so lucky to have the most inspirational mom! Thank you for showing

me what it means to work hard. Seeing you finish law school while working on my PhD has been a huge driving factor in getting me through my thesis.

Chapter 2, in full, is being prepared for submission for publication. Rebecca L Drake, Yang Sun, Alyssa M Collins, Caroline G Bullard, Van W Wong, Albert C Chen, William D Bugbee, Robert L Sah. The dissertation author is the primary investigator of this work.

VITA

2016 Bachelor of Science, Bioengineering, California Lutheran University

2018 Master of Science, Bioengineering, University of California San Diego

2022 Doctor of Philosophy, Bioengineering, University of California San Diego

ABSTRACT OF THE DISSERTATION

Centrifugal Cleansing of the Subchondral Bone of Osteochondral Grafts

by

Rebecca L Drake

Doctor of Philosophy in Bioengineering

University of California, San Diego, 2022

Professor Robert L Sah, Chair

Transplantation of an osteochondral allograft (OCA) is a generally effective treatment for large chondral or osteochondral lesions. The effectiveness of OCAs is enhanced by the removal of marrow from the subchondral bone and facilitated by the maintenance of viable chondrocytes. Cleansing of OC is currently performed by pulsatile fluid lavage alone or in combination with high-pressure gas/air, but limited by depth of removal, need for user manipulation, and collection and disposal of large volumes of cleansing fluid. Centrifugation is an alternative method that has been applied to massive, previously-frozen allografts, and large osteochondral fragments including whole femoral heads, but has not been studied for osteochondral cylinders (OCs).

The aim of the present study was to determine if centrifugation could be used to cleanse the marrow space of osteochondral cores (OCs) while maintaining viable chondrocytes. The effects of centrifugation duration (0-900 s) and centrifugal force (RCF, 0-10,000×g) were assessed on OCs from total knee arthroplasty (6 mm diameter, TKA) or OCA (8 mm diameter) tissue. Pellet

mass and OC mass were measured after centrifugation and after additional trypsin treatment to loosen residual marrow. OC trabecular bone and marrow structure was characterized quantitatively by micro-computed tomography (μCT), without and with Hexabrix contrast, and qualitatively by photography and histology. Chondrocyte viability was assessed by live/dead imaging.

Centrifugation at 10,000×g for 300s removed most of the marrow from TKA-OC based on estimates from pellet mass (88%) and μCT (73%), and from OCA-OC (72% and 86%, respectively). Release from TKA-OC was lower at 3,000xg/300s (64% and 45%) or shorter duration 10,000xg/30s (54%, pellet mass). The spatial variation in μCT images indicated that release progressed from the bone base up toward the subchondral plate. Release from OCA-OC was not affected by extending 10,000xg duration to 900s. Pellet mass correlated identically to OC mass decrease, and also correlated strongly with empty marrow volume by μCT. Histology with Oil Red O and Hematoxylin and Eosin confirmed the relative presence or absence of marrow. TKR and OCA donors differed in age (71 vs 20 yr), and their OC bone varied in volume faction (28% vs 38%), trabecular thickness (0.167 mm vs 0.188 mm), and trabecular separation (0.442 mm vs 0.371 mm). Chondrocyte viability throughout the cartilage was high for samples subjected to no centrifugation (95%) and only slightly diminished by 10,000xg centrifugation for 300 s (to 90%).

Centrifugation provides a method of cleansing OCs that is similarly effective as the current pulsatile lavage standard method in terms of marrow cleansing (~70%) while maintaining chondrocyte viability (~90%). Centrifugation provides a controlled treatment, avoiding manual manipulation with pulsatile lavage. Centrifugation also avoids the need to collect and dispose of large volumes of lavage fluid. Additionally, with pellet mass measurement, centrifugation allows a simple assessment of the degree of marrow cleansing. Finally, by varying centrifugation RCF and duration, the extent of cleansing can be varied.

Thus, centrifugation may provide a new effective method of cleansing OCAs that provides similar degrees of marrow cleansing and chondrocyte viability, while allowing convenient assessment by pellet mass and modulation of the degree of cleansing by varying RCF or duration.

CHAPTER 1. INTRODUCTION

1.1 Osteochondral Allograft Uses

The use of fresh osteochondral allografts (OCA) is a generally reliable and effective treatment for large chondral or osteochondral lesions, where the efficacy for treatment of the osteochondral lesions is well established clinically.[4,7,8,21] Causes for such lesions include osteochondral defects secondary to trauma, osteochondritis dissecans, osteonecrosis, and intra-articular fractures.[18,21] The grafting procedure is generally effective in restoring the joint surface with the structural integrity and stability needed for rehabilitation and return to activity.[4,7,34] Remodeling of the allograft occurs over several months, where creeping substitution of the host bone replaces the entire autograft with new tissue.[20] Fixation of grafts to the subchondral bone and surgical management of subchondral cysts beneath surface lesions are critical technical considerations that may affect graft success.[21] Sizing of the OCAs to have 4-10 mm of subchondral bone and matching of graft geometry to defects have been shown to enhances resistance to pullout and reduces subsidence, while cleansing OCAs to remove marrow elements and debris improves the bone incorporation of the graft.[21]

1.2 Factors Affecting OCA Effectiveness

1.2.1 Chondrocyte Viability

OCA survival depends on the viability of chondrocytes in the articular cartilage of the graft. Reduced chondrocyte cellularity in osteochondral allografts at the time of implantation is associated with poor graft survival at 12 months (**Fig. 1.1**).[10,22,40] The long-term efficacy of the graft is due, in part, to the presence of viable chondrocytes in the graft cartilage, which are able to

preserve homeostasis and prevent degeneration (**Fig. 1.2**).[40] The viability of chondrocytes within the cartilage can vary with graft storage, with frozen storage (-20ºC) killing cells, while refrigerated (4ºC) or incubation (37ºC) storage of allografts in various solutions is able to variably maintain cell viability.[39,40] In a canine model, the success of OCA repair was associated with >70% chondrocyte viability.[10] Histological analysis of early graft failures showed a lack of viable chondrocytes and cartilage and matrix staining in such grafts.[23]

1.2.2 Effective Subchondral Bone Remodeling

The effectiveness of OCAs depends on effective subchondral bone remodeling. Unlike the chondrocytes in the articular cartilage, the cells in the subchondral bone of fresh OCAs do not survive the refrigerated storage process,[46] so during remodeling, cells infiltrate from the host to the bone of the OCA.[11,19,41,42,44] Human bone is a metabolically active organ that undergoes continuous remodeling, where existing, damaged, or in this case foreign, bone is removed (bone resorption) and new bone is added (bone formation, **Fig. 1.3**).[14] In the case of OCA incorporation into a host, host cells repopulate and remodel the subchondral bone, gradually replacing the graft bone by creeping substitution. Both bone remodeling and creeping substitution are the result of action from the osteoblasts and osteoclasts that move along the bone to repair defects or fractures.[25] The osteoclasts move along the bone surface and resorb bone by acidification and proteolysis of the bone matrix.[25] The osteoblasts move in clusters following the osteoclasts and are responsible for the production of the new bone matrix.[25] Failure in the remodeling process often involve OCA subsidence with subchondral bone collapse (**Fig. 1.4**).[9,24,37]

1.3 Factors Affecting OCA Bone Repopulation and Remodeling

The success of OCA bone repopulation and remodeling by host cells depends on the osteoconductive, osteoinductive, and osteogenic characteristics of the graft. For a graft or construct to be osteoconductive, the tissue must allow for vascular invasion and cell infiltration.[38] The interconnectivity and pore size are especially important, as they not only provide support, but also allow transport of nutrients via cells and vasculature.[26,38] Although bone grafts and graft substitutes are inherently osteoconductive due to their native structure, they are often occluded with marrow that may block vascular and cell infiltration. Adipocytes, which are abundant in the bone marrow, normally regulate the balance between bone formation and resorption,[14] but when dead, as in the case of OCA at transplant, may also hinder cell recruitment from the host. Osteoinduction refers to the ability of a material to recruit and transform mesenchymal progenitor cells into mature, bone-forming osteoblasts.[26,36] For a material to be osteogenic, it must harbor cells that are capable of laying down new bone matrix within the tissue.[36] An OCA is thus osteoconductive and presumably somewhat osteoinductive, as is typical of bone graft, but not osteogenic since the indwelling bone cells do not survive the harvest and storage process. An OCA relies on recruitment of nearby cells (from the graft recipient) to remodel the grafted bone after placement.

1.4 Potential Benefits of OCA Cleansing

Effective cleansing of trabecular bone in OCAs potentially enhances graft incorporation not only by enhancing osteoconductivity, but also by reducing antigenicity. The marrow portion of bone grafts is antigenic,[29,53] so large, fresh cancellous allografts can elicit a vigorous immune response within the first two weeks after graft placement.[33] While OCA rejection is not an evident clinical problem, such immunogenicity may affect the integration of the graft with the host. This

type of an immunogenicity increases with graft size,[47,49,50] but can be minimized by OCA cleansing prior to placement.[21,29] Thus, the removal of marrow components reduces the potential of an immune response, while also enhancing the bone incorporation via increasing osteoconduction.[21,26,29,38]

1.5 Methods of OCA Bone Cleansing

The bone component of OCAs has been cleansed by three main strategies, chemical, thermal, and mechanical (**Table 1**). Chemical cleansing via the application of soaps, detergents, alcohols, and enzymes are widely used for bone grafts, but can damage cartilage, so are not common for use in OCAs.[15-17,31,48,55] Freezing or heating OCA may improve or facilitate marrow release, but they also are lethal to chondrocytes, so not used for OCA.[15-17,31,48,51,55] Thus, the most common methods for OCA cleansing are by mechanical force either by irrigation by fluid or gas/air or centrifugation, as these methods may locally affect the subchondral bone and leave the cartilage and chondrocytes intact.[35,51] For each of these methods, quantification of cleansing varies, as is described in subsequent text. Thus, qualitative descriptions of marrow removal—near 0 (0-5 % removal), low (5-15 %), relatively low (15-40 %), moderate (40-60 %), relatively high (60-80 %), high (80-95 %), and near complete (95-100 %)—are used.

1.5.1 Pulsed Lavage

Pulsatile lavage is the clinical standard for OCA cleansing, where pulses of high-pressured saline are directed at the subchondral bone to remove marrow components.[28] Cleansing may be performed on entire donor joints or on individual grafts. When used with osteochondral cores, a specialized irrigation tool that is manually oriented to direct fluid jets against the base of the OCA

is typically used. Controlled experimental protocols use ~1 L of saline over ~1 minute.[27,35] Suction ports help dispose of the saline-marrow mixture (**Figs. 1.5, 1.6**).[2] When cleansing by this method, the pressure of the saline wash is dependent on the distance between the nozzle and the marrow, whereby deeper marrow would be more difficult to remove.[32,45] Thus, an OCA is more thoroughly cleansed than an intact donor joint. The pulsed lavage method removes 61% of the marrow, based on empty marrow volume estimates by micro-computed tomography (μCT)), after 120 s of standard flow, and 78% after high flow.[51] Such irrigation predominantly removes marrow from the bone base and edges of the OCA, with marrow remaining in the deeper regions (closer to the subchondral bone plate) of the OCA.[51]

1.5.2 High Pressure Gas and Saline Irrigation

Bone cleansing by pressurized CO_2 gas has recently been combined with bulb irrigation or pulsatile lavage.[35] Both pressurized CO_2 gas and saline lavage involve the application of air or saline to the trabecular bone from a nozzle. The bulb syringe is a precursor to the pulsed lavage system, applying saline with less fluid pressure, thus having a lower cleansing efficacy (73 % cement intrusion/3 mm) as compared to standard pulsed lavage (87-92 % cement intrusion/3 mm).[28] In cleansing with CO_2 gas, the irrigation pressure is still related to the distance from the device nozzle to the marrow, although the local mechanics are likely different due to the distinct movement of air versus fluid through the trabecular bone network.[35] The marrow remaining in the superficial, middle, and deep bone regions (position relative to the exposed bone base) in 2D histological sections after combined pulsed saline lavage and CO_2 (30, 21, and 16 % marrow fill in deep, middle, and superficial zones) was less than those with pulsed saline lavage alone (59, 30, and 17 % fill). Assuming approximately 1/3 volume of each region, pulsed saline lavage removed

65 % ((41 % + 70 % + 83 %)/3) overall, whereas the combination of pulsed saline lavage and CO_2 removed 78 % (70 % + 79 % + 84 %)/3). These release percentages are similar to the empty marrow space volume percentages found by μCT, noted above, for standard-flow (61 %) and high-flow (78 %) pulsatile lavage.[51]

1.5.3 Centrifugation

Centrifugation may cleanse OCA marrow gradually throughout the trabecular bone, while also allowing for assessment of cleansing via pellet collection. As opposed to pulsed lavage, where irrigation pressure on OCA marrow varies with distance between the device nozzle and position of the marrow within the core, the force applied to marrow with centrifugation is governed by differences in density between particles.[1,32,45] The sedimentation of particles can be modeled by Stoke's law, where the sedimentation rate is proportional to the difference in density between the particle and the medium. Centrifugation of OCAs involves the stabilization of a graft within a tube, allowing applied force to separate marrow based on the density difference between the marrow and air. The difference in the densities of marrow (density of fat = 0.9 g/cm^3)[3] and air (0.0 g/cm^3)[54] allows the marrow to easily separate from an OCA as air fills its place.

OCA cleansing by centrifugation has previously been performed in whole femoral heads[16] and blocks cut from the distal femur and tibia (**Table 2**).[17] These methods of centrifugation have been able to achieve up to 99 % of marrow removal when used with additional sonication, wash, and alcohol treatments. [15-17,31,48,55] Though these additional treatments are suitable for bone grafts, they damage the cartilage. Thus, more extensive study on cleansing of osteochondral grafts, with core geometry, and localization of cleansing in OCAs could be beneficial.

1.6 Characterization of Marrow Removal

The removal of marrow from OCAs has traditionally been characterized by assessment of material disappearing from the OCA but might also be assessed by the mass released. Gross visualization of the OCA is often used in the clinic, but is only able to show marrow removal at the edge of the core, which does not allow for accurate approximation in central regions.[51] In joint resurfacing applications, the penetration of bone-cement is commonly used with radiograph or CT imaging for localization of cleansed regions, though it is difficult to determine if bone-cement is actually penetrating all empty spaces.[28] As noted above, histology is also used, destructively with samples, to assess release.[35] μCT is useful in identifying and localizing tissue structures in three dimensions at high resolution via the distinction of tissues by differences in x-ray absorption.[5,6,12] The use of contrast with μCT can help identify tissues that differ in adsorption of the contrast, allowing quantitation of cleansed marrow space.[30,43,51] Allograft mass change before and after cleansing has been used to give the percentage of allograft mass lost, though the method does not allow for localization of mass removal.[15-17,31,48] Combining non-destructive methods of mass release and μCT imaging, with destructive but detailed methods such as histology, could help delineate both the extent and patterns of marrow release for particular cleansing methods.

1.7 Synopsis

Cleansing of the bone component of OCAs potentially enhances the incorporation of the allograft for repair of osteochondral lesions by enhancing osteoconduction and possibly by reducing immunogenicity.[21,26,29,38] The amount of marrow removal needed to achieve these benefits is not fully understood and could be investigated with study of modulated marrow removal and its effects on graft survival. The most common method of cleansing the bone component of

allografts is by pulsed lavage, which is moderately effective and causes difficulty in quantifying cleansing because the removed material is dispersed.[28,32,45,51] This work seeks to evaluate centrifugation as an alternative method of OCA cleansing that also allows for modulation of the extent of release and also the convenient measurement of marrow removal.

1.8 Figures

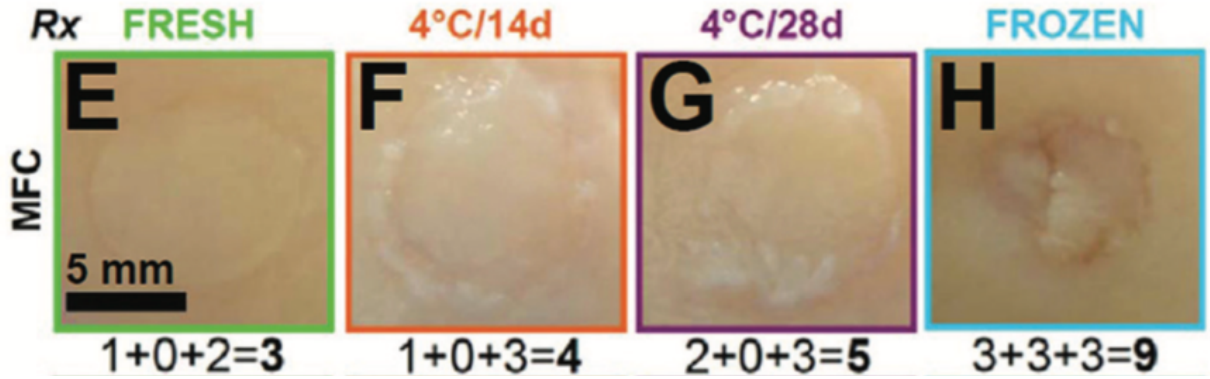

Figure 1.1. Structural analysis in retrieved allografts. (**A-D**) Gross macroscopic images of representative knee joints. (**E-L**) Individual retrieved FROZEN (blue), FRESH (green), 4C/14d (orange), and 4C/28d (purple) allografts at the medial femoral condyle (**E-H**) and lateral trochlea (**I-L**) sites. Gross scores (and components) are indicated below each representative image as surface 1 fill 1 integration = total. PROX, proximal; DIST, distal; MFC, medial femoral condyle; LT, lateral trochlea. (from [40])

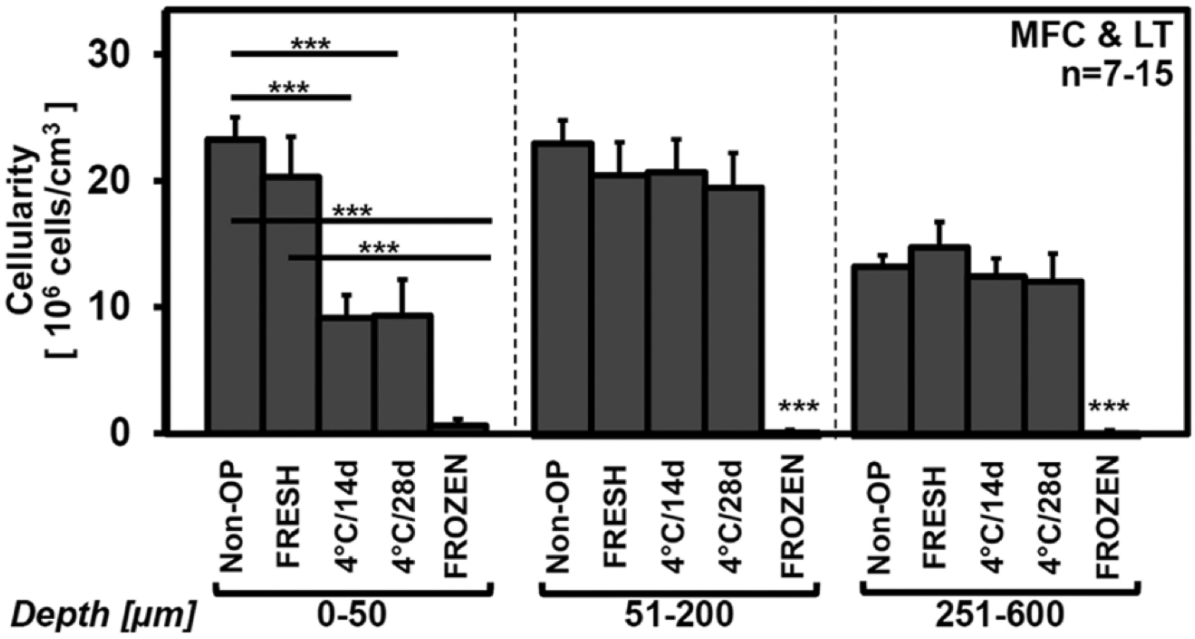

Figure 1.2. Effect of in vivo allograft storage on cellularity at selected depths from the articular surface. Bars represent mean & standard error of the mean. ***P \ .001. MFC, medial femoral condyle; LT, lateral trochlea; Non-OP, nonoperated controls. (from [40])

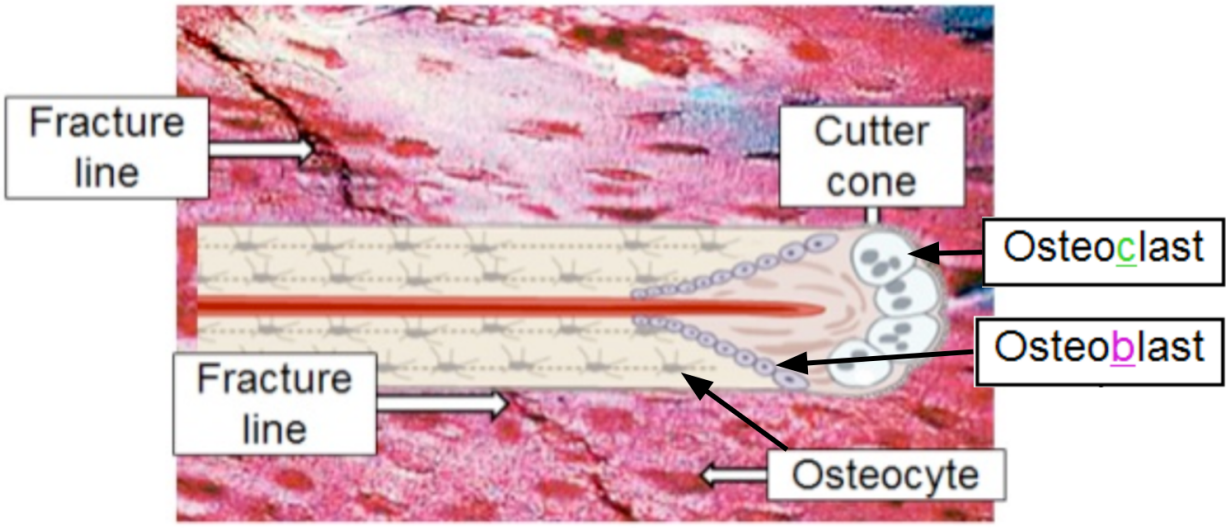

Figure 1.3. Schematic of fracture healing in bone. Osteoclasts move across fracture line, resorbing bone. Osteoblasts follow osteoclasts, forming new bone material.[13]

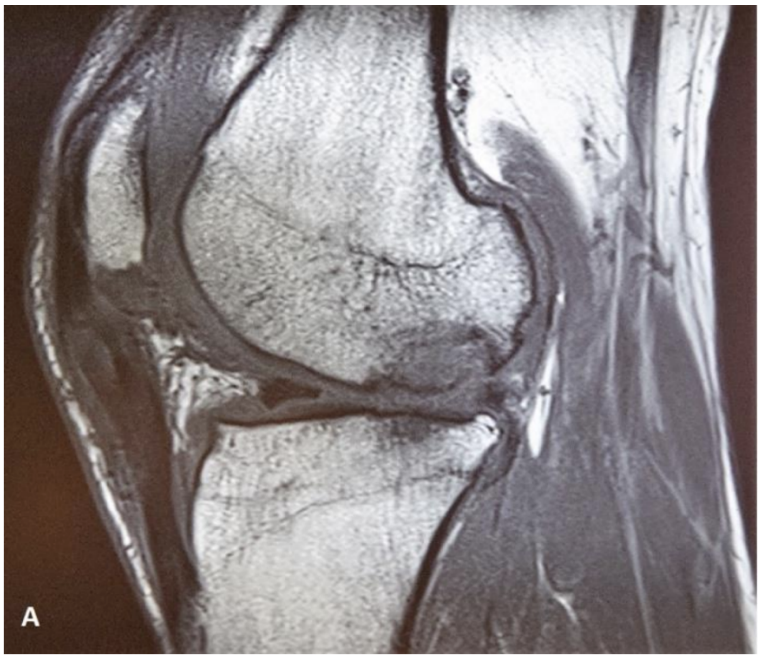

Figure 1.4. MRI of the right knee with complete graft failure. (**A**) sagittal T1 sequence and (**B**) coronal fluid sensitive sequence showing complete failure of the graft, diffuse cartilage wear and lateral meniscus deficiency. (from [34])

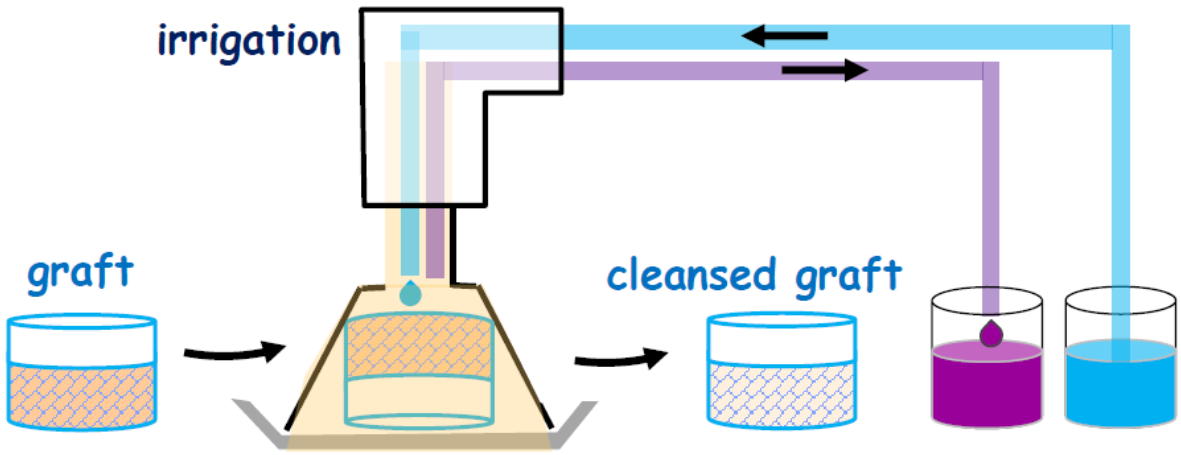

Figure 1.5. Schematic of pulsed lavage process. Nozzle fits to the base of an OCA and irrigates saline into the graft (blue), while excess saline and marrow is collected in a reservoir (purple).[52]

Figure 1.6. Pulsed lavage systems for total joint procedures. (**1**) Fully-disposable and (**2**) semi-disposable pulsed lavage systems for use in total joint procedures. Concurrent suction with soft cone splash shield for optimal fluid containment without damaging soft tissue. (from [2])

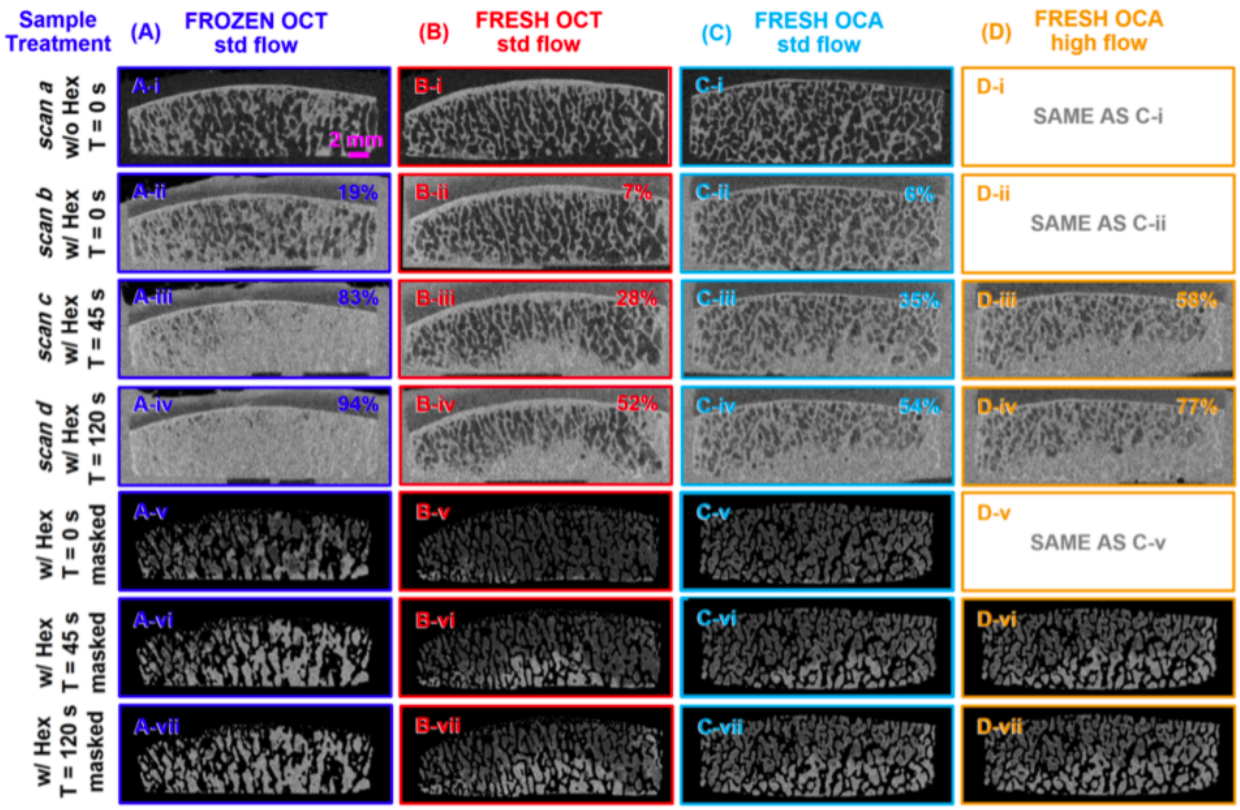

Figure 1.7. Representative µCT images of large contoured OCs after different storage and lavage treatments. Samples, (A) OCT/FROZEN, (B) OCT/ FRESH, (C, D) OCA/FRESH, were irrigated for (i, ii) 0 s, (iii) 45 s, and (iv) 120 s with (A, B, C) standard (std) flow or (D) high flow. Samples were imaged (i) without contrast or with Hexabrix contrast (ii) before and (iii, iv) after irrigation. (v, vi, vii) Post-treatment images (iii, iv, v) were masked to remove trabeculae and surrounding tissues and fluid. All sequential images (i-vii) were registered. (from [51])

Table 1.1. Previous studies of methods of marrow removal from human trabecular bone. Key papers itemized by study information related to samples, purpose, and methodology. NS = not stated. Cleansing type: T = thermal, C = chemical, M = mechanical. DZ = deep zone, MZ = middle zone, SZ = superficial zone.

Cit	Reference	Usage	Cleansing Type	Cleansing Method	Geometry	Storage	Health	Age Range (Avg) [yrs]
[28]	Kalteis, 2007	Endopros-thesis	T,M	Bulb syringe and pulsed lavage	Whole femoral heads	-20 °C, thaw o/n at RT	OA from THA	54-76 (62)
[51]	Sun, 2017	Osteo-chondral allograft	T,M	Pulsed lavage	Osteochondral cores (d = 20 mm, h = 3.5-6.5 mm)	-80 °C or 4 °C	OA from TKA and healthy	19-84 (65±14)
[35]	Meyer, 2017	Osteo-chondral allograft	T,M	Pulsed lavage and simultaneous saline and CO_2 lavage	Osteochondral cores (d = 15 mm, h = 6 mm)	NS	Healthy	NS
[16]	Eagle, 2018	Bone graft	C,T,M	Centrifugation with multiple sonication, wash, and ethanol steps	Whole femoral heads	-80 °C, thaw o/n at 4 °C	OA from THA and healthy	42-87

*Measured across 5 different pulsed lavage devices.

Table 1.1. Previous studies of methods of marrow removal from human trabecular bone, continued.

Cit	Reference	Sex (M/F)	Source	Quantification of Marrow Removal	Main Result
[28]	Kalteis, 2007	22/26	Femoral heads	% Bone-cement intrusion / 3 mm via CT	Bulb syringe: 73 % Pulsed lavage: 87-92 %*
[51]	Sun, 2017	9/8	Femoral condyles	% Hexabrix contrast infiltration into empty marrow space via μCT	Standard flow, fresh storage: 55 % empty marrow space after 120 s Standard flow, frozen storage: 92 % empty marrow space after 120 s High flow, fresh storage: 78 % empty marrow space after 120 s
[35]	Meyer, 2017	NS	Femoral condyles	% fill calculated from 2D histological sections	No lavage: 63 % DZ, 68 % MZ, 55 % SZ Pulsed lavage: 59 % DZ, 30 % MZ, 17 % SZ Saline + CO2 lavage: 30 % DZ, 21 % MZ, 16 % SZ
[16]	Eagle, 2018	1/5	Femoral heads	% removal bone marrow via presence of soluble protein and DNA in wash solutions	93-99 %

*Measured across 5 different pulsed lavage devices.

Table 1.2. Previous studies of centrifugation for use in removing marrow from human trabecular bone. Key papers itemized by study information related to samples, purpose, and methodology. NS = not stated.

Cit	Reference	Usage	Geometry	Storage	Health	Age Range [yrs]	Sex (M/F)	Source	RCF [×g]	Centrifuge Duration [min]
[55]	Wolfinbarger, 1999	Bone graft	Whole femoral heads	Frozen	Healthy	N/A	N/A	Femoral heads	1,200-3,500	10-20
[31]	Lomas, 2000	Bone graft	Whole femoral heads	48 h at -80 °C	Possible RA	55-82	3/3	Femoral heads	1,850	15
[48]	Smith, 2015	Bone graft	Whole femoral heads	-80 °C, thaw o/n at 5 °C	OA from THA	38-82	16/12	Femoral heads	1,850	15 ×3
[15]	Eagle, 2015	Bone graft	1 cm^3 cancellous cubes	-80 °C, thaw o/n at 4 °C	NS	38-50	1/2	Proximal tibia and distal femur	1,850	15 ×4
[17]	Eagle, 2017	Bone graft	Whole femoral heads	-80 °C, thaw o/n at 4 °C	NS	42-82	3/10	Femoral heads	1,850	15 ×3
[16]	Eagle, 2018	Bone graft	Whole femoral heads	-80 °C, thaw o/n at 4 °C	OA from THA and healthy	42-87	1/5	Femoral heads	1,850	15 ×3

Table 1.2. Previous studies of centrifugation for use in removing marrow from human trabecular bone, continued.

Cit	Reference	Additional Treatment
[55]	Wolfinbarger, 1999	Pulsed lavage, agitation, agitation, alcohol, and decontaminating agents.
[31]	Lomas, 2000	Multiple sonication and wash steps before and after centrifuging.
[48]	Smith, 2015	Multiple sonication, wash, and ethanol steps before and after centrifuging.
[15]	Eagle, 2015	Multiple sonication, wash, and ethanol steps before and after centrifuging.
[17]	Eagle, 2017	Multiple sonication, wash, and ethanol steps before and after centrifuging.
[16]	Eagle, 2018	Multiple sonication, wash, and ethanol steps before and after centrifuging.

1.9 References

1. Methods of Cell Separation: Elsevier; 1988.

2. MicroAire 5740 Disposable Pulse Lavage System. 2022. (Accessed at https://www.microaire.com/products/disposable-pulse-lavage-system.)

3. Abe T, Thiebaud RS, Loenneke JP: The mysterious values of adipose tissue density and fat content in infants: MRI-measured body composition studies. *Pediatr Res* 90:963-5, 2021.

4. Ahmed TA, Hincke MT: Strategies for articular cartilage lesion repair and functional restoration. *Tissue Eng Part B Rev* 16:305-29, 2010.

5. Bouxsein ML, Boyd SK, Christiansen BA, Guldberg RE, Jepsen KJ, Muller R: Guidelines for assessment of bone microstructure in rodents using micro-computed tomography. *J Bone Miner Res* 25:1468-86, 2010.

6. Brown K, Schluter S, Sheppard A, Wildenschild D: On the challenges of measuring interfacial characteristics of three-phase fluid flow with x-ray microtomography. *J Microsc* 253:171-82, 2014.

7. Bugbee W, Cavallo M, Giannini S: Osteochondral allograft transplantation in the knee. *J Knee Surg* 25:109-16, 2012.

8. Bugbee WD, Convery FR: Osteochondral allograft transplantation. *Clin Sports Med* 18:67-75, 1999.

9. Bugbee WD, Khanna G, Cavallo M, McCauley JC, Görtz S, Brage ME: Bipolar fresh osteochondral allografting of the tibiotalar joint. *J Bone Joint Surg Am* 95:426-32, 2013.

10. Cook JL, Stannard JP, Stoker AM, Bozynski CC, Kuroki K, Cook CR, Pfeiffer FM: Importance of donor chondrocyte viability for osteochondral allografts. *Am J Sports Med* 44:1260-8, 2016.

11. Cook JL, Stoker AM, Stannard JP, Kuroki K, Cook CR, Pfeiffer FM, Bozynski C, Hung CT: A novel system improves preservation of osteochondral allografts. *Clin Orthop Relat Res* 472:3404-14, 2014.

12. Demontiero O, Li W, Thembani E, Duque G: Validation of noninvasive quantification of bone marrow fat volume with microCT in aging rats. *Exp Gerontol* 46:435-40, 2011.

13. Bone anatomy and healing. (Accessed 2022, at https://aotrauma.aofoundation.org/-/media/project/aocmf/aotrauma/documents/education_pdf/orp_handout_english_bone-anatomy-and-healing.pdf.)

14. During A, Penel G, Hardouin P: Understanding the local actions of lipids in bone physiology. *Prog Lipid Res* 59:126-46, 2015.

15. Eagle MJ, Man J, Rooney P, Hogg P, Kearney JN: Assessment of an improved bone washing protocol for deceased donor human bone. *Cell Tissue Bank* 16:83-90, 2015.

16. Eagle MJ, Man J, Rooney P, Kearney JN: Comparison of bone marrow component removal from processed femoral head bone from living and deceased donors: presence of geodes in living donor bone can prevent maximum removal of marrow components. *Cell Tissue Bank* 19:727-32, 2018.

17. Eagle MJ, Man J, Rooney P, McQuillan TA, Galea G, Kearney JN: Assessment of a closed wash system developed for processing living donor femoral heads. *Cell Tissue Bank* 18:547-54, 2017.

18. Familiari F, Cinque ME, Chahla J, Godin JA, Olesen ML, Moatshe G, LaPrade RF: Clinical outcomes and failure rates of osteochondral allograft transplantation in the knee: A systematic review. *Am J Sports Med* 46:3541-9, 2018.

19. Glenn RE, Jr., McCarty EC, Potter HG, Juliao SF, Gordon JD, Spindler KP: Comparison of fresh osteochondral autografts and allografts: a canine model. *Am J Sports Med* 34:1084-93, 2006.

20. Goldberg VM: Natural history of autografts and allografts. In: *Bone implant grafting,* ed. by Springer, London, 1992, 9-12.

21. Gortz S, Bugbee WD: Allografts in articular cartilage repair. *Instructional Course Lectures* 56:469-80, 2007.

22. Görtz S, Tabbaa SM, Jones DG, Polousky JD, Crawford DC, Bugbee WD, Cole BJ, Farr J, Fleischli JE, Getgood A, Gomoll AH, Gross AE, Krych AJ, Lattermann C, Mandelbaum BR, Mandt PR, Mirzayan R, Mologne TS, Provencher MT, Rodeo SA, Safir O, Strauss ED, Wahl CJ, Williams RJ, Yanke AB: Metrics of OsteoChondral Allografts (MOCA) group consensus statements on the use of viable osteochondral allograft. *Orthop J Sports Med* 9:2325967120983604, 2021.

23. Gross AE, Kim W, Las Heras F, Backstein D, Safir O, Pritzker KP: Fresh osteochondral allografts for posttraumatic knee defects: long-term followup. *Clin Orthop Relat Res* 466:1863-70, 2008.

24. Gross AE, Shasha N, Aubin P: Long-term followup of the use of fresh osteochondral allografts for posttraumatic knee defects. *Clin Orthop Relat Res* 435:79-87, 2005.

25. Hadjidakis DJ, Androulakis, II: Bone remodeling. *Ann N Y Acad Sci* 1092:385-96, 2006.

26. Hak DJ: The use of osteoconductive bone graft substitutes in orthopaedic trauma. *J Am Acad Orthop Surg* 15:525-36, 2007.

27. Hirn MY, Salmela PM, Vuento RE: High-pressure saline washing of allografts reduces bacterial contamination. *Acta Orthop Scand* 72:83-5, 2001.

28. Kalteis T, Pforringer D, Herold T, Handel M, Renkawitz T, Plitz W: An experimental comparison of different devices for pulsatile high-pressure lavage and their relevance to cement intrusion into cancellous bone. *Arch Orthop Trauma Surg* 127:873-7, 2007.

29. Lewandrowski KU, Rebmann V, Päßler M, Schollmeier G, Ekkernkamp A, Grosse-Wilde H, Tomford WW: Immune response to perforated and partially demineralized bone allografts. *J Orthop Sci* 6:545–55, 2001.

30. Li X, Anton N, Zuber G, Vandamme T: Contrast agents for preclinical targeted X-ray imaging. *Adv Drug Deliv Rev* 76:116-33, 2014.

31. Lomas R, Drummond O, Kearney JN: Processing of whole femoral head allografts: a method for improving clinical efficacy and safety. *Cell Tissue Bank* 1:193-200, 2000.

32. Luedtke-Hoffmann KA, Schafer DS: Pulsed lavage in wound cleansing. *Phys Ther* 80:292-300, 2000.

33. Markel MD: Bone Grafts and Bone Substitutes. In: *Equine Fracture Repair,* ed. by AJ Nixon, Wiley-Blackwell, 2020, 163-72.

34. Marom N, Bugbee W, Williams RJ: Osteochondral grafts failures. *Oper Tech Sports Med*, 2019.

35. Meyer MA, McCarthy MA, Gitelis ME, Poland SG, Urita A, Chubinskaya S, Yanke AB, Cole BJ: Effectiveness of lavage techniques in removing immunogenic elements from osteochondral allografts. *Cartilage* 8:369-73, 2017.

36. Miron RJ, Zhang YF: Osteoinduction: a review of old concepts with new standards. *J Dent Res* 91:736-44, 2012.

37. Oakeshott RD, Farine I, Pritzker KPH, Langer F, Gross AE: A clinical and histologic analysis of failed fresh osteochondral allografts. *Clin Orthop Relat Res* 233:283-94, 1988.

38. Özcan M, Hotza D, Fredel MC, Cruz A, Volpato CAM: Materials and manufacturing techniques for polymeric and ceramic scaffolds used in implant dentistry. *J Compos Sci* 5:78, 2021.

39. Pallante AL, Bae WC, Chen AC, Gortz S, Bugbee WD, Sah RL: Chondrocyte viability is higher after prolonged storage at 37 degrees C than at 4 degrees C for osteochondral grafts. *Am J Sports Med* 37 Suppl 1:24S-32S, 2009.

40. Pallante AL, Chen AC, Ball ST, Amiel D, Masuda K, Sah RL, Bugbee WD: The in vivo performance of osteochondral allografts in the goat is diminished with extended storage and decreased cartilage cellularity. *Am J Sports Med* 40:1814-23, 2012.

41. Pallante AL, Gortz S, Chen AC, Healey RM, Chase DC, Ball ST, Amiel D, Sah RL, Bugbee WD: Treatment of articular cartilage defects in the goat with frozen versus fresh osteochondral allografts: effects on cartilage stiffness, zonal composition, and structure at six months. *J Bone Joint Surg Am* 94:1984-95, 2012.

42. Pallante-Kichura AL, Cory E, Bugbee WD, Sah RL: Bone cysts after osteochondral allograft repair of cartilage defects in goats suggest abnormal interaction between subchondral bone and overlying synovial joint tissues. *Bone* 57:259–68, 2013.

43. Palmer AW, Guldberg RE, Levenston ME: Analysis of cartilage matrix fixed charge density and three-dimensional morphology via contrast-enhanced microcomputed tomography. *Proc Natl Acad Sci U S A* 103:19255-60, 2006.

44. Ranawat AS, Vidal AF, Chen CT, Zelken JA, Turner AS, Williams RJ, 3rd: Material properties of fresh cold-stored allografts for osteochondral defects at 1 year. *Clin Orthop Relat Res* 466:1826-36, 2008.

45. Rodeheaver GT, Pettry D, Thacker JG, Edgerton MT, Edlich RF: Wound cleansing by high pressure irrigation. *Surg Gynecol Obstet* 141:357-62, 1975.

46. Rodrigo JJ, Thompson E, Travis C: Deep-freezing versus 4° preservation of avascular osteocartilaginous shell allografts in rats. *Clin Orthop Relat Res* 218:268-75, 1987.

47. Sirlin CB, Brossmann J, Boutin RD, Pathria MN, Convery FR, Bugbee W, Deutsch R, Lebeck LK, Resnick D: Shell osteochondral allografts of the knee: comparison of mr imaging findings and immunologic responses. *Radiology* 219:35-43, 2001.

48. Smith CA, Richardson SM, Eagle MJ, Rooney P, Board T, Hoyland JA: The use of a novel bone allograft wash process to generate a biocompatible, mechanically stable and osteoinductive biological scaffold for use in bone tissue engineering. *J Tissue Eng Regen Med* 9:595-604, 2015.

49. Stevenson S: The immune response to osteochondral allografts in dogs. *J Bone Joint Surg Am* 69-A:573-82, 1987.

50. Strong DM, Friedlaender GE, Tomford WW, Springfield DS, Shives TC, Burchardt H, Enneking WF, Mankin HJ: Immunologic responses in human recipients of osseous and osteochondral allografts. *Clin Orthop Relat Res* 326:107-14, 1996.

51. Sun Y, Jiang W, Cory E, Caffrey JP, Hsu FH, Chen AC, Wang J, Sah RL, Bugbee WD: Pulsed lavage cleaning of osteochondral grafts depends on lavage duration, flow intensity, and graft storage condition. *PLoS One* 12:e0176934, 2017.

52. Sun Y, Tabbaa SM, Jiang W, Hsu FH, Wong VW, Chen AC, Cheng W, Bugbee WD, Sah RL: Pulsed lavage cleansing of osteochondral grafts depends on bone thickness and irrigation duration. *Trans Int Cart Repair Soc*, 2016.

53. VandeVord PJ, Nasser S, Wooley PH: Immunological responses to bone soluble proteins in recipients of bone allografts. *J Orthop Res* 23:1059-64, 2005.

54. Williams NR: The calculation of air density in various units. *Bull Am Meteorol Soc* 30:319–20 1949.

55. Wolfinbarger Jr L, Ford L: Process for cleaning bone grafts using centrifugal force and bone grafts produced therebyUnited States Patent # 5,977.432, 1999.

CHAPTER 2. CLEANSING OF OSTEOCHONDRAL CORES BY CENTRIFUGATION DEPENDS ON CENTRIFUGE FORCE AND DURATION

2.1 ABSTRACT

Background. Osteochondral allograft (OCA) is a generally effective treatment for large chondral or osteochondral lesions. The effectiveness of OCAs is enhanced by the removal of marrow from the subchondral bone and facilitated by the maintenance of viable chondrocytes. Centrifugation may provide a new method for effectively removing marrow from OCAs.

Aims. The aims of the present study were to determine if centrifugation could be used to cleanse the marrow space of osteochondral cores (OCs) while maintaining viable chondrocytes.

Methods. The effects of centrifugation duration (0-900 s) and centrifugal force (RCF, 0-10,000×g) were assessed on OCs from total knee arthroplasty (6 mm diameter, TKA) or OCA (8 mm diameter) tissue. Pellet mass and OC mass were measured after centrifugation and after additional trypsin treatment to loosen residual marrow. OC trabecular bone and marrow structure was characterized quantitatively by micro-computed tomography (μCT), without and with Hexabrix contrast, and qualitatively by photography and histology. Chondrocyte viability was assessed by live/dead imaging.

Results. Centrifugation at 10,000×g for 300s removed most of the marrow from TKA-OC based on estimates from pellet mass (88±8%) and μCT (73±11%), and from OCA-OC (72±11% and 86±2%, respectively). Release from TKA-OC was lower at 3,000xg/300s (64±11% and 45±14%) or shorter duration 10,000xg/30s (54±7%, pellet mass). The spatial variation in μCT images indicated that release progressed from the bone base up toward the subchondral plate. Release from OCA-OC was not affected by extending 10,000xg duration to 900s. Pellet mass correlated

identically to OC mass decrease, and also correlated strongly with empty marrow volume by μCT. Histology with Oil Red O and Hematoxylin and Eosin confirmed the relative presence or absence of marrow. TKR and OCA donors differed in age (71 vs 20 yr), and their OC bone varied in volume faction (27.8% vs 38.3%), trabecular thickness (0.167 mm vs 0.188 mm), and trabecular separation (0.442 vs 0.371 mm). Chondrocyte viability throughout the cartilage was high for samples subjected to no centrifugation (95±2%) and only slightly diminished by 10,000xg centrifugation for 300 s (90±2%).

Discussion/Conclusion. Centrifugation provides a method of cleansing OCs that is similarly effective as the current pulsatile lavage standard method in terms of marrow cleansing (~70%) while maintaining chondrocyte viability (~90%). Centrifugation provides a controlled treatment, avoiding manual manipulation with pulsatile lavage. Centrifugation also avoids the need to collect and dispose of large volumes of lavage fluid. Additionally, with pellet mass measurement, centrifugation allows a simple assessment of the degree of marrow cleansing. Finally, by varying centrifugation RCF and duration, the extent of cleansing can be varied.

Statement of clinical significance. Thus, centrifugation may provide a new effective method of cleansing OCAs that provides similar degrees of marrow cleansing and chondrocyte viability, while allowing convenient assessment by pellet mass and modulation of the degree of cleansing by varying RCF or duration.

2.2 INTRODUCTION

Transplantation of an osteochondral allograft (OCA) is a generally reliable and effective treatment for large chondral or osteochondral lesions. Repair effectiveness depends, in part, on OCA stabilization at the graft site, by primary healing of bone between implant and host.[3,7,19,28,35,45,52] For treatment of large osteochondral lesions (>2 cm^2 diameter) or bone involvement (>5-9 mm depth), 85% and 74% graft survival was seen at 10 and 15 years, respectively.[2,6] The main steps of the process are recovery, testing, and storage of a donor joint and then preparation of the donor graft for the recipient in the operating room.[9] These procedures restore the joint surface with the structural integrity and stability of an osteochondral graft which allows the application of loads early in the post-operative period, a faster rehabilitation and faster return to activity.[34] OCA subsidence with subchondral bone (ScB) collapse may be an indication of failure during this post-operative period.[8,24,37] The marrow portion of bone allografts is antigenic[29,51] and can elicit an immune response after transplantation, where induction of humoral immunity increases with the size of the graft.[46,48,49] Though cells in the ScB of fresh OCA stored at 4℃ do not survive the storage process,[44] the bone structure is preserved and acts as a graft for where the bone cells are replaced during remodeling of the allograft over several months.[14,18,20] During remodeling, primary bone repair by creeping substitution of the host bone replaces the donor bone with new tissue.[11,20,21,39,40,42] Cleansing of allografts functions to remove marrow including the abundant adipose cells from the trabecular bone of the graft. This cleansing enhances bone integration into the host via improved osteoconduction.[22,26,29,47]

The bone component of OCAs has been cleansed according to two main physical principles, an applied pressure applied at the base of the sample, or a force acting on the whole sample (**Table S1**). Pulsatile lavage is the standard method used for cleansing with the use of high-

pressure PBS cleansing of the trabecular bone.[27] The irrigation pressure diminishes with distance between the device nozzle and the OCA.[33,43] The pressure also diminishes with increased distance within the marrow, so that deeper marrow (closer to the subchondral bone plate) experiences less pressure and is more problematic to dislodge. Cleansing with high pressure air or gas is somewhat similar,[36] although the details of air versus fluid mechanics within the subchondral bone will differ. The second physical approach is centrifugation, where the force applied to the marrow is governed by differences in component density (**Table S2**).[1] The sedimentation of particles can be modeled by Stoke's law, where the sedimentation rate is proportional to the difference in density between the particle and the medium. In this process, the bone may be held in place, and marrow is easily removed from an OCA as it is denser than the air (medium), which would fill its place. Few studies exist to assess the efficacy of centrifugation in removing marrow from fresh, unfrozen OCA ScB.

Marrow cleansing has been assessed previously using morphological, mechanical, and biochemical measurements. Gross visualization is often used in the clinic and gives an approximation of the extent of marrow removal at the edge of the sample but does not give information about the center. Allograft mass change before and after cleansing has also been useful in giving the percentage of allograft mass loss, but may reflect mass lost throughout the sample.[15-17,32,47] Use of radiograph or CT imaging to assess the penetration of bone-cement is common for joint resurfacing applications as the bone-cement is radiopaque, allowing for easy localization of the cleansed regions.[27] The bone-cement functions well in localization, but it is unclear if the bone-cement infiltrates fully into all regions of marrow removal. Micro-computed tomography (μCT) is useful for identifying and localizing mineralized tissue structures at high resolution and in three dimensions,[4] readily distinguishing between bone, fluid, and fat due to differences in X-ray absorption.[5,12] When used with Hexabrix (Hex) contrast agent, μCT can provide both visualization

and quantitation of a cleansed marrow space, where the contrast is able to help identify tissues that differ in adsorption of contrast.[31,41,50] This method provided localization and quantitation of marrow cleansing of OCAs (without damage to the graft) via the pulsed-lavage cleansing but similar quantitation has yet to be applied to centrifugal cleansing. **Fig. 1** illustrates a workflow with output measures.

The aims of the present study were to determine the effectiveness of centrifugation in cleansing marrow space on osteochondral cores (OCs). For total knee replacement OCs (TKR-OCs) and OCA-OCs, the effectiveness of centrifugation was evaluated for different (i) centrifugation intensities and (ii) durations, in terms of (A) marrow removal by imaging and histology, and (B) maintenance of chondrocyte viability. In addition, the differences in cleansing of TKR-OCs and OCA-OCs and relationship to bone microstructure were assessed.

2.3 METHODS

2.3.1 Study Design

The effects of centrifugation duration (0-300 s) and centrifugal force (RCF, 0-10,000×g) on the location and extent of OC marrow cleansing was assessed on human samples from total knee arthroplasty remnants. 45 OCs (d = 6 mm, h = 5 mm) were prepared and distributed amongst four groups (**Fig. 1, Table TS1**): (1) negative control--no centrifugation (n = 13), (2) centrifugation at 1,000×g (n = 6), (3) centrifugation at 3,000×g (n = 6), and (4) centrifugation at 10,000×g (n = 14), Live/Dead and histological imaging (n = 6). Samples from groups 2-4 were centrifuged sequentially for a total of 10, 30, 100, and 300 s. Then (as a positive control), samples of all groups were incubated with 1 mL of 0.25 % tissue culture grade trypsin for 15 min and subsequently centrifuged at 10,000×g for 300 s. The mass of each OC (with its support) and pellet (in its

centrifuge tube) was taken initially and after each period of centrifugation (**Table TS2**). The samples were also photographed and imaged by μCT for qualitative and quantitative characterization of bone structure. Imaging by μCT was performed initially (without contrast), after initial 300 s of centrifugation (without and then after equilibration with contrast), and after final centrifugation (after equilibration with contrast). Selected samples were used for live/dead imaging (n = 3 per group) or histology (n = 2 per group) with Oil Red O (ORO) and Hematoxylin and Eosin (H&E).

From the mass measures of the samples, the supports, and the empty centrifuge tubes, calculations were made for the initial OC weight (m^{OC}_0), differences in OC weight from the initial weight ($m^{OC}_{RCF,t-0}$), and pellet weights ($m^{P}_{RCF,t-0}$). From μCT data, images of each OC sample were processed for bone volume, total volume, bone volume relative to total volume (BV/TV), trabecular bone thickness (Tb.Th), and trabecular bone separation (Tb.Sp), the total volume of subchondral bone (ScB.V), volume of bone trabeculae (Tb.V), and volume of contrast-infiltrated marrow space (Hex.V).[13] The images of live cells and of dead cells were processed to calculate live cell density, dead cell density, and the percentage of viable cells. The relationship between decrease in core mass and increase in pellet mass with centrifugation for various RCFs and durations were assessed by linear regression. The effects of RCF and duration on cleansing efficacy ($m^{OC}_{RCF,t}$ and $m^{P}_{RCF,t}$, before trypsin) were analyzed via two-way repeated measures ANOVA and one-way ANOVA for each duration with post-hoc Tukey test. The effects of 300 s RCF on the extent of cleansing was assessed by comparing pre-trypsin and post-trypsin (cleansing control) states by two-way repeated measures ANOVA and t-test for each duration. The effects of bone morphology parameters (BV/TV, Tb.Th, and Tb.Sp) on cleansing efficacy (by mass and

volume) were analyzed for TKR-OCs and OCA-OCs (grouped by tissue source and together) were assessed by one-way ANOVA with post-hoc Tukey test at the terminal centrifuge time point.

The effects of centrifugation for removing marrow in OC samples was assessed on human samples prepared from OCA remnants. 9 OCs (d = 8 mm, h = 5 mm) were prepared and centrifuged sequentially at 3,000×g for 300, 600, and 900 s and at 10,000×g for 300 s. The mass of each OC (with its support) and pellet (in its centrifuge tube) was taken initially and after each period of centrifugation. The samples were also photographed and imaged by μCT for qualitative and quantitative characterization of bone structure. Imaging by μCT was performed initially (without and then after equilibration with contrast), after 900 s of centrifugation at 3,000×g (after equilibration with contrast), and after final centrifugation (after equilibration with contrast). Mass measures and μCT data were processed as was done for initial measurements for 6 mm OCs.

2.3.2 Osteochondral Samples

OCs (6 or 8 mm diameter, 5 mm subchondral bone length)[9] were harvested from femoral condyles of discarded knee fragments from patients undergoing total knee replacement (TKR) surgery, n = 45 (6 mm samples) and cadaveric tissue bank donors, n = 9 (8 mm samples); harvesting received institutional review board approval. OA cores were harvested within 24 h of surgery and graded by visual inspection as having no or partial erosion of the cartilage (18 patients, 6 male, 12 female, 70 ± 9 years). Tissue bank donor cores were processed for 21-24 days at the tissue bank prior to surgery and harvested within 17-35 days of surgery and graded by visual inspection as having no erosion of the cartilage (4 patients, all male, 20 ± 2 age). TKR fragments were used after storage at 4 ºC for 1-2 days in a mixture of 10% Dulbecco's Modified Eagle's Medium and 90 % phosphate-buffered saline (PBS). OC samples were prepared to a diameter of

6 mm with a 7 mm allograft donor harvester from the Osteochondral Autograft Transfer System (Arthrex, Naples, Florida) and stored 4 ºC thereafter, except when centrifuging and scanning. The cores were stored overnight (14-16 hours) in PBS supplemented with 100 U/mL penicillin, 100 µg/mL streptomycin, and 0.25 µg/mL fungizone (PBS+PSF). Then, the core was trimmed at the base with an oscillating saw (Stryker, Kalamazoo, Michigan) to leave a 4-5 mm length of bone. OCs used were screened to ensure intact articular cartilage, integrity of the subchondral bone, and straightness of the OC.

OCs from cadaveric tissue bank donors are referred to as OCA, since they are identical to those used clinically. OCA samples were prepared to a diameter of 8 mm with an 8 mm allograft coring reamer (Arthrex, Naples, Florida); the coring reamer was used for the OCA samples to account for the harder bone. While being cored, an osteochondral fragment was irrigated with PBS to dissipate heat. The cores were stored (1-2 weeks) at 4 ºC in PBS+PSF. Then, the core was trimmed at the base with an oscillating saw to leave a 5 mm length of bone.

2.3.3 Centrifugation

TKR-OCs were centrifuged at varying RCF and subsequently imaged and weighed to analyze marrow removal. OCs were centrifuged in 1.5 mL microfuge tubes at 1,000, 3,000, or 10,000×g repeatedly for a total of 10, 30, 100, and 300 s. OCs were gently pat dry with a kimwipe prior to centrifugation to remove excess droplets while maintaining moisture in the cartilage. Gross images were taken initially and after the final centrifugation to demonstrate the OC and pellet. Mass of the OC and pellet were determined initially and after 10, 30, 100, and 300 s of centrifugation. The difference between initial sample or container mass and the final mass was taken as an index of the marrow removal.

For positive control samples, OCs were centrifuged at 10,000×g and then subjected to a trypsin treatment with additional centrifugation for 300 s at 10,000×g to remove any remaining marrow (T + 10,000×g). For the trypsin treatment, OCs were rehydrated via placement in a syringe containing ~3 mL of PBS with the application of negative pressure to remove air pockets. Rehydrated OCs were placed in 1 mL of 0.25 % tissue culture grade trypsin (Gibco/Invitrogen, Waltham, Massachusetts) for 15 min at 4 ºC to allow for diffusion of the trypsin into the OC and then transferred to a tube rotator at room temperature for 15 min. The OC was placed in 10 % fetal bovine serum (FBS) in PBS and then centrifuged at 10,000×g for 300 s. Gross images were taken pre- and post-centrifugation, and also post-trypsin treatment, of the OC and pelleted output. Mass of the OC and pelleted output were taken as repeated measures initially, after 10, 30, 100, and 300 s of centrifugation, and T+10,000×g, to assess marrow removal. Mass measures of the OC and pelleted output were normalized by the pellet mass after trypsin treatment.

OCA-OCs were centrifuged at varying RCF and subsequently imaged and weighed to analyze marrow removal. OCs were centrifuged in 2 mL cryovials at 3,000 or 10,000×g repeatedly for a total of 300, 600, and 900 s at 3,000×g and an additional 300 s at 10,000×g. Gross images were taken initially, after 900 s of centrifugation at 3,000×g, and after the final centrifugation to demonstrate the OC and pellet. Mass of the OC and pellet were determined initially and after 300, 600, and 900 s at 3,000×g and an additional 300 s at 10,000×g centrifugation. The difference between initial sample or container mass and the final mass was taken as an index of the marrow removal.

2.3.4 Viability

Throughout centrifugation and scanning procedures, care was taken to minimize manipulations that would diminish cartilage viability. The samples were stored in PBS before and after centrifugation. In preparation for centrifugation, the cartilage surfaces were gently dabbed to remove excess fluid with a moist Kimwipe. During centrifugation and μCT scanning the samples were within a capped container to maintain a humid environment. Cartilage exposure to air and drying were minimized during initial gross imaging, initial weighing, and weighing after repeated centrifugation. The total duration of exposure cartilage to air (not including time in a capped tube) was <1 min.

Viability and cellularity were assessed at the articular surface, depthwise, and near the circumferential edge in OCs with Live / Dead staining. Each OC was cut vertically in half and stained with 2.67 μM calcein-AM and 5 μM ethidium homodimer-1 (LIVE/DEAD™ Viability/Cytotoxicity Kit; Molecular Probes, Eugene, Oregon) in culture medium (Dulbecco's Modified Eagle Medium + 10 % Fetal Bovine Serum) for 15-20 min at 37 °C and rinsed in phosphate-buffered saline solution for five minutes. The samples were imaged with a fluorescence microscope (Eclipse TE300; Nikon, Melville, New York), a mercury arc lamp (Nikon HB10103AF), G-2A (for "dead" images; Nikon) or B-2A (for "live" images; Nikon) filter cubes, a Plan Fluor 10× objective lens (NA = 0.3; Nikon), and an AmScope camera ($(317\ \mu m)^2$ /px, FOV = 1.56 mm x 1.17 mm; United Scope LLC, Irvine, California) at central and edge regions. Each disk was imaged en face and at the cut vertical surface over an area of 90 μm^2 and a depth of ~200 μm beyond the surface in order to see past cells affected by the blade. Images were analyzed for the number of live, dead, and total cells within regions that contain ~100 cells to achieve adequate cell sampling. To sample similarly radially and depthwise, central regions were analyzed in 300 x

300 μm^2 regions, whereas edges were analyzed in 450 x 200 μm^2 regions so as to represent the edge region that would be influenced by the coring reamer or razor blade. Live and Dead cell numbers within the image areas were counted manually, and the percentage of live cells was computed.

2.3.5 Histology

The correspondence of features in histology and μCT images were assessed. 8 OCs were prepared from two TKR donors (62 and 63 years old M) and distributed amongst four groups (**Fig. 1, Table TS1**): (1) negative control—no centrifugation (n = 2), (2) centrifugation at 3,000×g (n = 2), (3) centrifugation at 10,000×g (n=2), and (4) centrifugation at 10,000×g for 300 s followed by incubation with trypsin for 15 min and subsequent centrifugation at 10,000×g for 300 s (n = 2). The samples were processed for histology by fixing with 4% paraformaldehyde in PBS for 72-96 hr, rinsing in PBS for 72 hr, and bisecting through the central vertical plane. Half of the OC was stained with 0.6% Oil Red O in water (ORO) and imaged grossly and by fluorescence microscopy. The other half of the OC was decalcified with formic acid (TBD-2, Fisher Scientific, Pittsburgh, Pennsylvania) for 72 hr and were embedded in paraffin, stained with Hematoxylin and Eosin (H&E), and slide scanned. H&E and ORO images were then compared to assess the relationship between marrow content and centrifugation.

2.3.6 μCT

OCs were μCT scanned following centrifugation to assess marrow removal. Samples were μCT scanned in PBS prior to centrifugation (*scan a*), to maintain hydration in the cartilage of the OC, then scanned again in Hex after centrifugation (300 s total) and rehydration of the sample and

equilibration in 20 % Hex in PBS (*scan b*), and finally after T+10,000×g rehydration of the sample and equilibration in 20 % Hex in PBS (*scan c*). In all scans, samples were held in a 2 mL microcentrifuge tube with a circumferential tube support or styrofoam holding the OC in place within the microcentrifuge tube. Samples were rehydrated via placement of the sample in PBS with application of negative pressure to remove air pockets. Each incubation in Hex-containing bath solution was at 4 °C for 24 h (duration calculated as τ, from the radius of an OC and diffusivity of a 3,000 Da solute diffusing into intact bone, $\tau = l^2/D = (3\ mm)^2/(10\text{-}4\ mm^2/s))$[30] to ensure equilibration and improved visualization of empty marrow spaces. Imaging was performed with a μCT scanner (Skyscan 1076, Bruker, Kontich, Belgium) at $(18\ \mu m)^3$ voxel resolution, applying electric potential of 100 kVp and a current of 100 μA, using 0.038 mm copper + 0.05 mm aluminum filters.[50]

2.3.7 Image Visualization and Analysis

For each sample, μCT images were visualized as 2D cross-sections and analyzed in areas of interest (AOIs) for Hex penetration into the marrow spaces. μCT datasets were displayed as three orthogonal 2D (3OV) images with two vertical and one horizontal cross-sections intersecting at the center of the subchondral bone region. An AOI was defined within each image to be 0.5 mm from the bottom and circumferential edges and at the bottom edge of the subchondral bone plate. This resulted in two rectangular AOIs and one circular AOI. Following a presentation template, sample images and ID were inserted. Then, Hex infiltration within the AOIs were initially estimated by visually comparing to standard sample images representative of 0, 10, 30, 50, 70, 90, and 100 % Hex infiltration and the value was noted for each vertical cross-section on the slide.

These visual estimates were used as checks against quantitative values, determined from image processing as described below.

To determine sample changes between states, imagesets were registered to match translation and rotation of the initial scan (*scan a*). Imagesets were cropped from registered (*scan a*) normal and (*scan b-c*) post-centrifugation volumes to encompass the entire OC. The post-centrifugation scans were registered and cropped using DataViewer v1.5.4.6 [Bruker, Kontich, Belgium]. The full registered volumes were saved and subsequently cropped to a 700x700x700 voxel (~12.3x12.3x12.3 mm^3) VOI for d = 6 and 8 mm OCs.

For each sample, *scan a* was processed to define a cylindrical volume of interest (VOI) containing most of the ScB, including trabecular bone (TB) and marrow volume (Ma.V). From *scan a*, bone was segmented by thresholding, using a gray scale value midway between the average gray scale values of bone and of marrow. The VOI was set to span axially from the basal bone surface to the subchondral plate, and radially outwards to a diameter of 5 mm and a height of 3 mm (0.5 mm from the circumferential edge and base); this was achieved by creating a mask, beginning with the segmented bone, dilating, eroding, applying a shrink-wrap in 3D to close the trabecular space, and then applying a circumferential erosion in 2D.

Scan a was analyzed within the VOI for bone volume, total volume, bone volume relative to total volume (BV/TV), trabecular bone thickness (Tb.Th), and trabecular bone separation (Tb.Sp). Scans *a-c* were then analyzed within the VOI for empty marrow space (volume), EMa. V, relative to Ma.V. For each sample, the total volume of marrow space, Ma.V within the VOI, was defined by masking out the bone (determined in scan a) expanded by one voxel to account for partial volume effects. Within the marrow space, EMa.V was then determined as voxels with gray scale values and distribution similar to that of the Hex-containing solution surrounding the sample

using Excel (Microsoft, Redmond, WA). Empty marrow volume fraction was then calculated as EMa.V/Ma.V. To illustrate the bone and marrow structure of individual samples, vertical cross-section images from *scans a-c* were displayed.

2.3.8 Statistical Analysis

The following general statistical procedures were followed. Data of individual experimental groups is presented as mean ± SE. Percentage data were log10 transformed before ANOVA or t-test. Statistical significance was set at $\alpha = 0.05$.

The effects of centrifuge force and duration on cleansing efficacy (by mass and volume) were analyzed for TKR-OCs. First, the effects of centrifuge force and duration were assessed by two-way repeated measures ANOVA. When the effects of centrifuge force were significant, their effect at each centrifuge time point was assessed by one-way ANOVA with post-hoc Tukey test. Comparisons of cleansing efficacy pre- and post-trypsin treatment groups and RCF were analyzed by two-way ANOVA and Dunnett's multiple comparison post-hoc test.

The effects of centrifuge force and extended time on cleansing efficacy (by mass and volume) were analyzed for OCA-OCs. The effects of extended time (300, 600, 900s) were assessed by one-way repeated measures ANOVA with post-hoc Tukey test. When the effects of extended time were not significant, the final time point at 3,000×g RCF was assessed with 300 s at 10,000×g RCF by one-way repeated measures ANOVA with post-hoc Tukey test.

The effects of centrifuge force (0 or 10,000xg for 300s) on percentage cell viability in TKR-OCs were analyzed by t-test. The effects were assessed separately for *en face*, superficial/middle (S/MZ), and deep zones (DZ). The effects were also assessed for averaged *en*

face with S/MZ and DZ by one-way ANOVA and also for an overall average (en face with S/MZ and DZ).

Patient (TKR) and donor (OCA) characteristics, age and bone morphology parameters (BV/TV, Tb.Th, and Tb.Sp), were compared by t-test.

The effects on cleansing efficacy (mass and volume metrics) of bone morphology parameters (BV/TV, Tb.Th, and Tb.Sp) were analyzed for TKR-OCs and OCA-OCs (separately by tissue source, and also together) by linear regression. For pellet mass, the combined analysis of TKR-OCs and OCA-OCs were performed by scaling OCA-OC mass down by the relative cross-sectional areas of TKR-OC to OCA-OC.

2.4 RESULTS

2.4.1 Effect of centrifugation on appearance of OC and pellet

Marrow removal from OCs appeared sensitive to centrifugation for 300s and at 10,000×g based on gross images of OCs (**Fig. 2A-J**) and pelleted output (**Fig. 2K-O**). Without centrifugation, the ScB of the OCs was pink overall, with small ~0.5 mm wide areas that were light-pink, consistent with marrow space, and thinner, irregular white structures, consistent with bone trabeculae (**Fig. 2A-E**). After 300 s of centrifugation at 10,000×g, areas extending from the bottom edge were white-light pink, with some remaining pink near the bone-cartilage interface (**Fig. 2G-J**). In parallel, the pellet of the OCs appeared to have greater volume with increasing RCF. For samples centrifuged at 1,000, 3,000, and 10,000×g, the pellet had three distinct layers—(1) a superficial, clear, yellow fluid, (2) a clear fluid, and within the clear fluid was (3) a red, opaque, solid (**Fig. 2L-N**). For samples treated with trypsin and subsequently centrifuged, a smaller red, opaque solid was present, surrounded by clear, pink fluid (**Fig.2O**).

Marrow removal from OCA-OCs also appeared sensitive to centrifugation for 300 s at 10,000×g based on gross images of the OCs (**Fig. 9A-E**) and pelleted output (**Fig. 9F-J**). Without centrifugation, the ScB of the OCs was beige overall, with small ~0.5 mm wide areas that were yellow-beige, consistent with marrow space, and thinner, irregular white structures, consistent with bone trabeculae. After 300 s of centrifugation at 3,000×g, areas extending from the bottom edge were white-light yellow, with some remaining yellow-beige near the center and bone-cartilage interface. After 600 and 900 s of centrifugation at 3,000×g, OCs appeared similar to that of 300 s with areas extending from the bottom edge were white-light yellow. After 300s of centrifugation at 10,000×g, areas extending from the bottom edge were white-light yellow, with little remaining yellow-beige near the bone-cartilage interface. In parallel, the pellet of the OCs appeared to have greater volume with increasing RCF. The three pellet layers, appeared similar to those of the TKR-OCs. The pellet did not have a detectable difference in volume with extended centrifugation time at 3,000×g. Thus, the macroscopic appearance of samples indicated cleansing extended toward the bone-cartilage interface with high (10,000×g) RCF.

2.4.2 Effects of centrifuge force and duration on the location and extent of marrow removal in OC samples

Registered μCT images of OCs (*scan a* and *c*) showed spatial patterns after centrifugation at different forces (**Fig. 3**) that were consistent with the qualitative photos (**Fig. 2**). In the ScB of the uncentrifuged sample, without Hex contrast (**Fig. 3A**), trabeculae were evident as thin irregular (~0.1-0.3 mm thick) bright stripes, with marrow evident as interspersed dark areas. Visible above the ScB was the subchondral plate, a bright horizontal strip (~0.2-0.5 mm thick). With Hex contrast (*scan c*, **Fig. 3F-J**), the ScB trabeculae and marrow regions were variably brightened, as compared

to the initial scans of the sample. In 0×g and 1,000×g groups, brightening was localized to the base and circumferential edges of the sample. In 3,000×g, 10,000×g, and T+10,000×g groups, samples were increasingly bright throughout the ScB with few darkened regions in the central region of the sample.

The pellet mass, an index of absolute (**Fig. 4A**) and normalized (**Fig. 4C**) marrow release resulting from centrifugation, of TKR-OCs was affected by RCF ($p < 0.001$) and duration ($p < 0.001$), with interaction ($p < 0.01$, **Fig. 4A**). After 300s, the pellet mass varied with RCF ($p < 0.001$) being higher (50.7 mg, $p < 0.001$) at 10,000×g and (41.5 mg, $p < 0.005$) at 3,000×g, respectively, than that (15.7 mg) at 1,000×g. In contrast, the overall (T+10,000×g) marrow release (averaging 58-67 mg), after trypsin treatment and 10,000×g RCF for 300 s, was not affected by the preceding centrifugation RCF ($p = 0.64$, **Fig. 4B**), and used as a sample-specific normalization. Normalized pellet mass (**Fig. 4C**) followed trends similar to absolute pellet mass (**Fig. 4A**), being affected by RCF ($p < 0.001$) and duration ($p < 0.001$), with interaction ($p < 0.01$), with absolute and normalized pellet mass increasing with RCF intensity and duration. Thus, after 300s RCF, the normalized pellet mass indicated nearly complete marrow release (88 %) at 10,000×g, high marrow release (64 %) at 3,000×g, and slight release (25 %) at 1,000×g.

The pellet mass, an index of absolute (**Fig. 11A**) and normalized (**Fig. 11C**) marrow release resulting from centrifugation, of OCA-OCs was affected by RCF ($p < 0.01$), without a detectable effect with extended time ($p = 0.21$). After repeated centrifugation for a total of 1,200 s, the pellet mass varied with RCF ($p < 0.01$), being higher (98.6 mg, $p < 0.01$) after 300 s at 10,000×g than that (79.8 mg) after 900 s at 3,000×g. In contrast, the marrow release (averaging 72.9-79.8 mg) at 3,000×g, was not affected by extended duration of centrifugation for a total of 600 or 900 s ($p = 0.24$, **Fig11A**). Normalized pellet mass (**Fig. 11C**), with sample-specific normalization by the

volume of the trabecular bone according to the height of the sample, followed trends similar to absolute pellet mass (**Fig. 11A**), being affected by RCF ($p < 0.01$), without detectable effect with extended time ($p = 0.21$). Thus, the normalized pellet mass indicated nearly complete marrow release (72.1 %) after 300 s of centrifugation at 10,000×g and high marrow release (64.4 %) after 900 s at 3,000×g.

Quantitative image analysis of TKR-OCs confirmed that absolute (**Fig. 8B**) and normalized (**Fig. 8D**) marrow removal, as indicated by % Hex infiltration into empty marrow space, was affected by RCF ($p < 0.001$). After 300s, the empty marrow volume varied with RCF ($p < 0.001$), being higher (27.8 mm^3, $p < 0.005$) at 10,000×g and (19.9 mm^3, $p = 0.29$) at 3,000×g, respectively, than that (9.7 mm^3) at 1,000×g or without centrifugation (5.0 mm^3). In contrast, the controlled (T+10,000×g) marrow release (36.1 mm^3) after trypsin treatment and 10,000×g RCF for 300 s, was similar to that at 10,000×g. Normalized empty marrow space (**Fig. 8D**) followed trends similar to absolute empty marrow space (**Fig. 8B**), being affected by RCF ($p < 0.001$), with absolute and normalized empty marrow space increasing with RCF intensity. Thus, after 300 s RCF, the normalized empty marrow space indicated relatively high marrow release (72.8 %) at 10,000×g, moderate marrow release (45.2 %) at 3,000×g, and relatively low release (24.6 %) at 1,000×g.

Quantitative image analysis of OCA-OCs confirmed that absolute (**Fig. 14B**) and normalized (**Fig. 8C**) marrow removal, as indicated by % Hex infiltration into empty marrow space, was affected by RCF ($p < 0.005$). Much like TKR-OCs after 900 s at 3,000×g or 300 s at 10,000×g, the empty marrow volume varied with RCF ($p < 0.005$), being higher (53.7 mm^3, $p < 0.05$) at 10,000×g and (42.1 mm^3, $p < 0.05$) at 3,000×g, respectively, than without centrifugation (7.5 mm^3). Normalized empty marrow space (**Fig. 8D**) followed trends similar to absolute empty marrow space (**Fig. 8B**), being affected by RCF ($p < 0.001$), with absolute and normalized empty

marrow space increasing with RCF intensity. Thus, after 300 s RCF, the normalized empty marrow space indicated high marrow release (86.2 %) at 10,000×g, moderate marrow release (74.5 %) at 3,000×g, and relatively low release (18.1 %) at 0×g.

2.4.3 Effects of centrifugation on fat staining

Qualitative images with ORO staining supported that marrow was removed by centrifugation, as indicated by reduced reddening of the marrow regions after centrifugation (**Fig. 6**). In gross images of OC halves without staining (**Fig. 6A-C**), certain features were evident for different RCF values. Without centrifugation, the ScB of the OCs were yellow overall, with small ~0.5 mm wide areas that were yellow, consistent with marrow space, and thinner, irregular white structures, consistent with bone trabeculae. With 10,000×g and also with T + 10,000×g groups, described above, areas extending from the bottom edge were white-light yellow, with some remaining yellow near the bone-cartilage interface. In gross images with ORO staining (**Fig. 6D-F**), other features were evident for the different RCF values. Without centrifugation, the ScB of the OCs was red overall, with ~0.5 mm wide areas that were bright red, consistent with stained marrow space, and thinner, irregular dark red structures, consistent with stained bone trabeculae. With 10,000×g and T + 10,000×g groups, areas extending from the bottom edge were dark red, with some bright red spaces remaining near the bone-cartilage interface. In fluorescent images with ORO staining (**Fig. 7A,C,E, S3**), similar features were seen without centrifugation where ~0.5 mm wide areas stained bright red, consistent with ORO-stained fat, surrounded by unstained irregular structures, consistent with bone trabeculae. With 10,000×g and T + 10,000×g groups, little reddening appeared in marrow regions as compared to those of uncentrifuged samples. Thus,

the bright red staining of marrow regions appears lessened in centrifuged samples as compared to uncentrifuged OCs.

Qualitative images of OCA-OCs with ORO staining supported that marrow was removed by centrifugation, as indicated by reduced reddening of the marrow regions after centrifugation (**Fig. 12**). In gross images of OC halves without staining (**Fig. 12A-C**), certain features were similarly evident in OCA and TKR-OCs (**Fig. 6A-C**). Without centrifugation, the ScB of the OCs were yellow overall, with small ~0.5 mm wide areas that were yellow, consistent with fatty marrow, as is typical of the distal half of long bones.[25] Thinner, irregular white trabecular structures bordered the yellow regions. In gross images with ORO staining (**Fig. 6D-F, 12D-F**), other features were evident after the different RCFs. Without centrifugation, the ScB of the OCs was red overall, with ~0.5 mm wide areas that were bright red, consistent with stained marrow space, and thinner, irregular pink structures, consistent with stained bone trabeculae. With 10,000×g and T + 10,000×g groups, areas extending from the bottom edge were dark red, with some bright red spaces remaining near the bone-cartilage interface and center of the OC. With T+10,000×g groups, OCs appeared pink overall in OCA samples as compared to TKR samples that appeared dark red, consistent with lessened staining of bone in OCA samples. In fluorescent images with ORO staining (**Fig. 7A,C,E, 13A,C,E**), similar features were seen without centrifugation where ~0.5 mm wide areas stained bright red, consistent with ORO-stained fat, surrounded by unstained irregular structures, consistent with bone trabeculae. With 10,000×g and T + 10,000×g groups, little reddening appeared in marrow regions of OCA-OCs as compared to those of uncentrifuged samples, where 10,000×g samples had dark red staining throughout marrow spaces and T+10,000×g samples had dark red staining on the edges of trabeculae. Thus, the bright red staining

of marrow regions appears lessened in OCA-OCs in centrifuged samples as compared to uncentrifuged OCs.

2.4.4 Effects of centrifugation on cell viability

Cell viability throughout the bulk of the OC was high initially and after centrifugation (**Fig. 5**). In *en face* images, the typical pattern of cells in pairs and strings was evident, with viability being high (99±1%, n=3) for the 0xg group and also high (90±1%, n=3) for the 10,000×g group, with a slight reduction ($p<0.01$). In the vertical section images, cells had the expected depth variation typical of articular cartilage, with the superficial zone showing cells in a relatively high density and orientation parallel to the surface, and the deep zone showing cells at a lesser density and oriented perpendicular to the surface and subchondral plate. In these vertical sections, superficial/middle zone chondrocyte viability was 95±2% for the 0xg group and 88±6%, for the 10,000×g group, without a distinguishable difference ($p=0.34$), and deep zone chondrocyte viability was 92±4% for both the 0xg and the 10,000×g group ($p=1.00$).

2.4.5 Effects of bone morphology on marrow release

The patient and donor ages for TKR and OCA samples, as well as their subchondral bone properties, differed (**Table 1**). Compared to OCA samples, the TKR samples were older, had less dense bone with lower BV/TV, lower trabecular thickness, and higher trabecular spacing.

There were certain correlations between marrow removal parameters and subchondral bone properties. Absolute pellet mass (**Fig. 11A**), marrow release resulting from centrifugation, of TKR-OCs was affected by trabecular separation ($p < 0.05$), and also BV/TV ($p < 0.05$) and trabecular thickness ($p < 0.001$) within the OCA-OCs (**Table 1, Fig. S4-6**). Pellet mass, absolute and

normalized, appeared to vary, though not significantly, with BV/TV ($p = 0.08$ and 0.06, respectively), being higher with lesser bone volume. Similarly, the absolute pellet mass varied with trabecular separation ($p < 0.05$), being lower with lesser trabecular separation and higher. The pellet mass and empty marrow space were not affected by the trabecular thickness ($p = 0.96$, 0.18, and 0.19 for absolute and normalized pellet mass and empty marrow space, respectively).

2.5 DISCUSSION

These results demonstrate that centrifugation cleansing of OC by is fast and effective, also allowing for quantification of marrow removal. Other methods of OC cleansing, namely pulsed lavage, can achieve marrow cleansing in a similar timeframe (2-5min), but require a specialized tool and do not allow for quantification of the marrow removed.[33] Centrifugation resulted in cleansing that used a common laboratory instrument and materials and Centrifugation was quantifiable by both the mass of the marrow removed (**Figs. 4, 14**) and by visualization of the cleansing depth (**Figs. 2, 3, 9, 10**).[1] Marrow cleansing of each of the groups increased sequentially with centrifuge force and longer durations of centrifugation. Visually, the marrow clearance started at the sample base and progressed upwards. The location of cleansing within the OCs was not quantified, but could be assessed in the future by defining regions radially and with depth in the sample and performing similar quantification of EMa.V/Ma.V for the defined regions.

The present study was designed to allow study of a number of human samples from both OCA and TKR remnants due to the scarcity of OCA remnants and ready availability of discarded fragments from TKR surgery with relatively preserved articular cartilage. In addition, most samples were tested repeatedly, at 0, 10, 30, 100, and 300 s or 0, 300, 600, 900, and 1,200 s (900 +300 s) of centrifugation time, both to conserve samples and to increase the power of elucidating

differences between time points. Relatively small, 6 mm TKR samples and 8 mm OC samples were used for an initial assessment of the effects of RCF and duration due to the limited size of the fragments and the limited OCA remnants. In the future, OC samples representative of clinical samples, up to 30 mm diameter and subchondral bone lengths ranging from 3-10 mm edge height, could be evaluated.[9] At the center of larger grafts, the thickness of the subchondral bone would be substantially greater than the bone height at the circumferential edge.

The use of OCs from two sources allowed for variation in bone morphometry that affected the marrow release. BV/TV and trabecular thickness yielded more marrow release with larger bone volume and trabecular thickness, while marrow release was less with larger trabecular separation.

The use of contrast-enhanced μCT allowed visualization and localization of the initial and remaining marrow. As would be expected, marrow released began at the sample base and progressed upwards (**Fig. 3, 10**). Some volumes with retained marrow appeared to be bounded below by horizontal bone struts. Additional studies could examine the release pattern in more detail.

The present study took particular care to maintain hydration of the articular cartilage to minimize detrimental effects on cell viability. Even at high RCF (10,000×g), chondrocyte viability could be maintained at high levels (~90 %) in TKR specimens. Viability was not assessed in OCA samples because they were subjected to repeated bouts of centrifugation, and also, as discarded tissue handled to prepare clinical OCA, it is likely that the tissue surface was somewhat compromised. Since the viability was maintained in superficial, middle, and deep zones of the cartilage are well over 70%, the long-term efficacy of a graft cleansed by centrifugation is promising.[10,23,38] In the future, more detailed chondrocyte functionality should be assessed to provide a more comprehensive examination of the possible effects of centrifugation.

The present study developed centrifugation for use in removing marrow from OCAs using common laboratory materials and a desktop centrifuge. The measurement of marrow removal via the pellet mass allows for sample-specific quantification of cleansing that can be quickly measured or estimated visually. The extent of marrow release by centrifugation, 73±11 % cleansing of TKR and 86±2 % of OCA, is comparable to the 65% marrow removal via standard pulsed saline lavage and 78 % marrow removal by combination pulsed saline and CO_2 lavage.[36]

The gradual and controlled release of marrow from OCs during centrifugation at various RCF and duration extend the previous studies on large tissue segments, and have implications for potential applications. Previous studies used centrifugation for removing marrow and blood components from massive allograft (93-99 % removal of marrow components, methods not clearly specified), previously frozen femoral heads for ~15 min at 1,850×g.[15-17,32,47] The present study showed that the centrifuge duration could be substantially less for OCs with the use of higher RCF. Centrifugation conditions to achieve intermediate amounts of marrow release may be useful to assess the ideal amount of marrow cleansing for graft effectiveness.

Chapter 2, in full, is being prepared for submission for publication. Rebecca L Drake, Yang Sun, Alyssa M Collins, Caroline G Bullard, Van W Wong, Albert C Chen, William D Bugbee, Robert L Sah. The dissertation author is the primary investigator of this work.

2.6 FIGURES

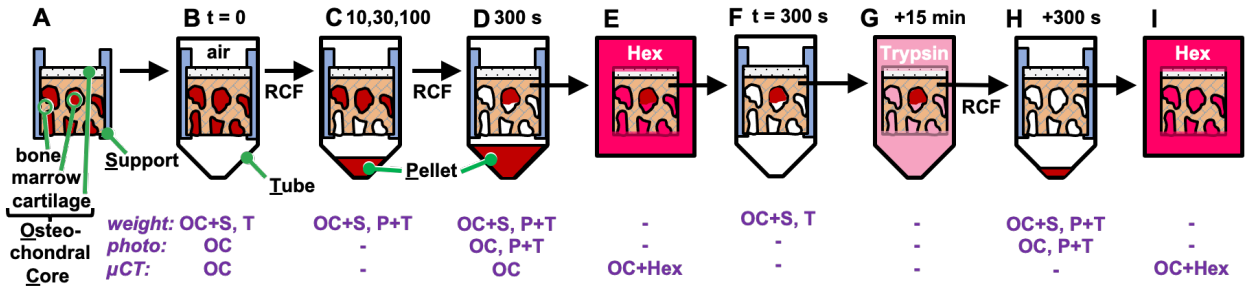

Figure 2.1. Procedure to analyze effect of centrifugation on marrow removal from Osteochondral Core (OC). (**A**) OC (bone, cartilage, and marrow) within a circumferential Support (S). (**B-D,F,H**) OC+S in centrifuge Tube (T). (**C-D,H**) OC+S with Pellet (P) in T after being subjected to centrifugal force (RCF) from time (**B**) t=0 to (**C**) 10 s, 30 s, or 100 s, and then to (**D**) 300 s, and for (**H**) an additional 300 s after (**G**) digestion with Trypsin. (**E,I**) OC equilibrated with 20% Hex in PBS (Hex). Weight, photo, and μCT taken at indicated states (**B-I**).

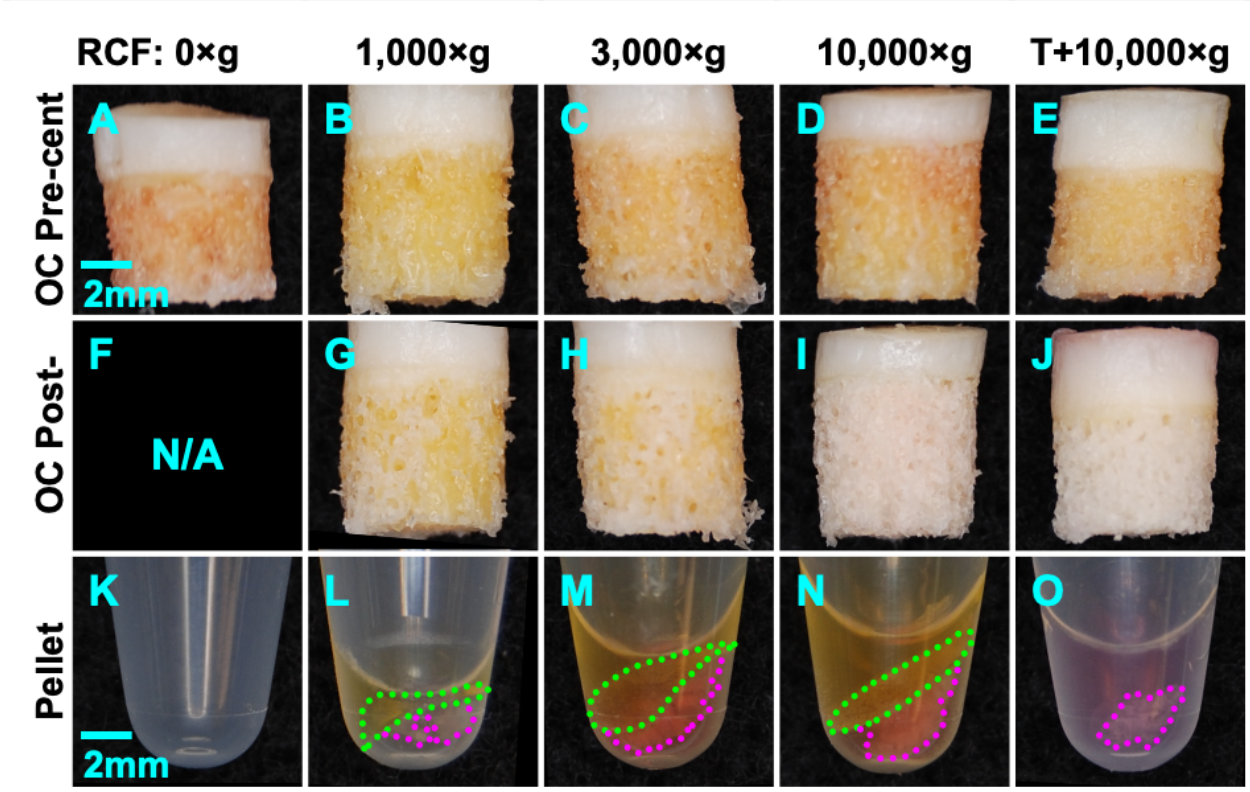

Figure 2.2. Representative gross images of TKR-OCs after centrifugation at different forces. Images of gross core appearance (**A-E**) before and (**F-J**) after centrifugation for 300 s at varying RCF with (**K-O**) pellet at base of centrifuge tube.

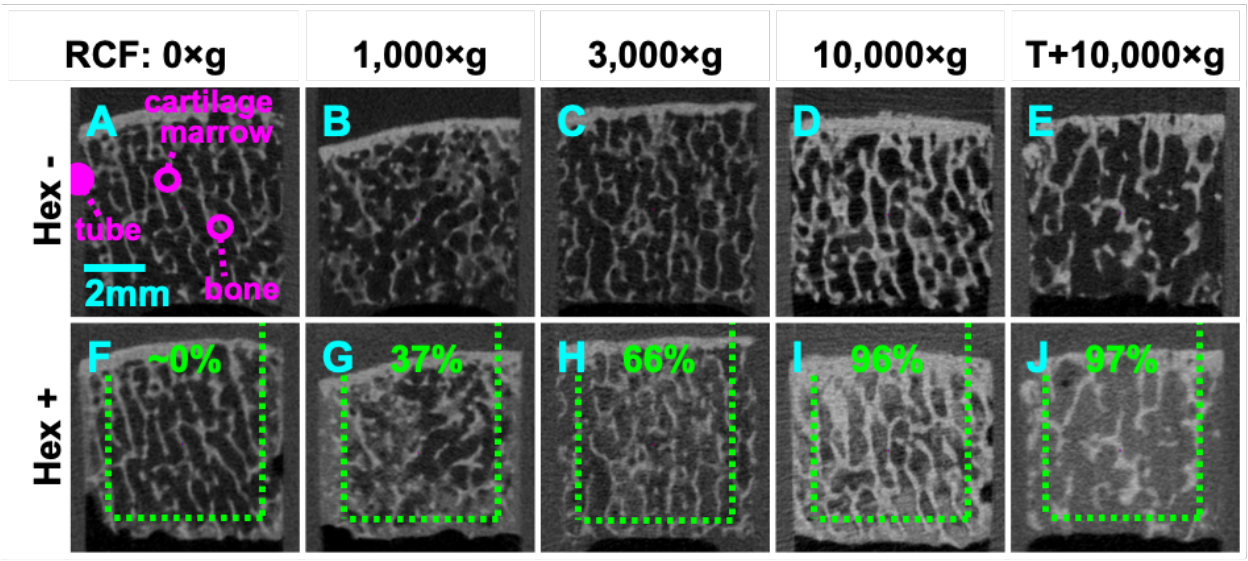

Figure 2.3. Representative µCT images (2D slices) of TKR-OCs after centrifugation. Samples centrifuged for 300 s at (**A,F**) 0, (**B,G**) 1,000, (**C,H**) 3,000, (**D,I**) 10,000×g, and (**E,J**) trypsin treatment before 10,000×g RCF (T+10,000×g). Samples imaged (**A-E**) pre-centrifugation without contrast or (**F-J**) post-centrifugation after equilibration with Hex contrast (Hex). Image analysis was for region bounded by dotted green line and subchondral plate above.

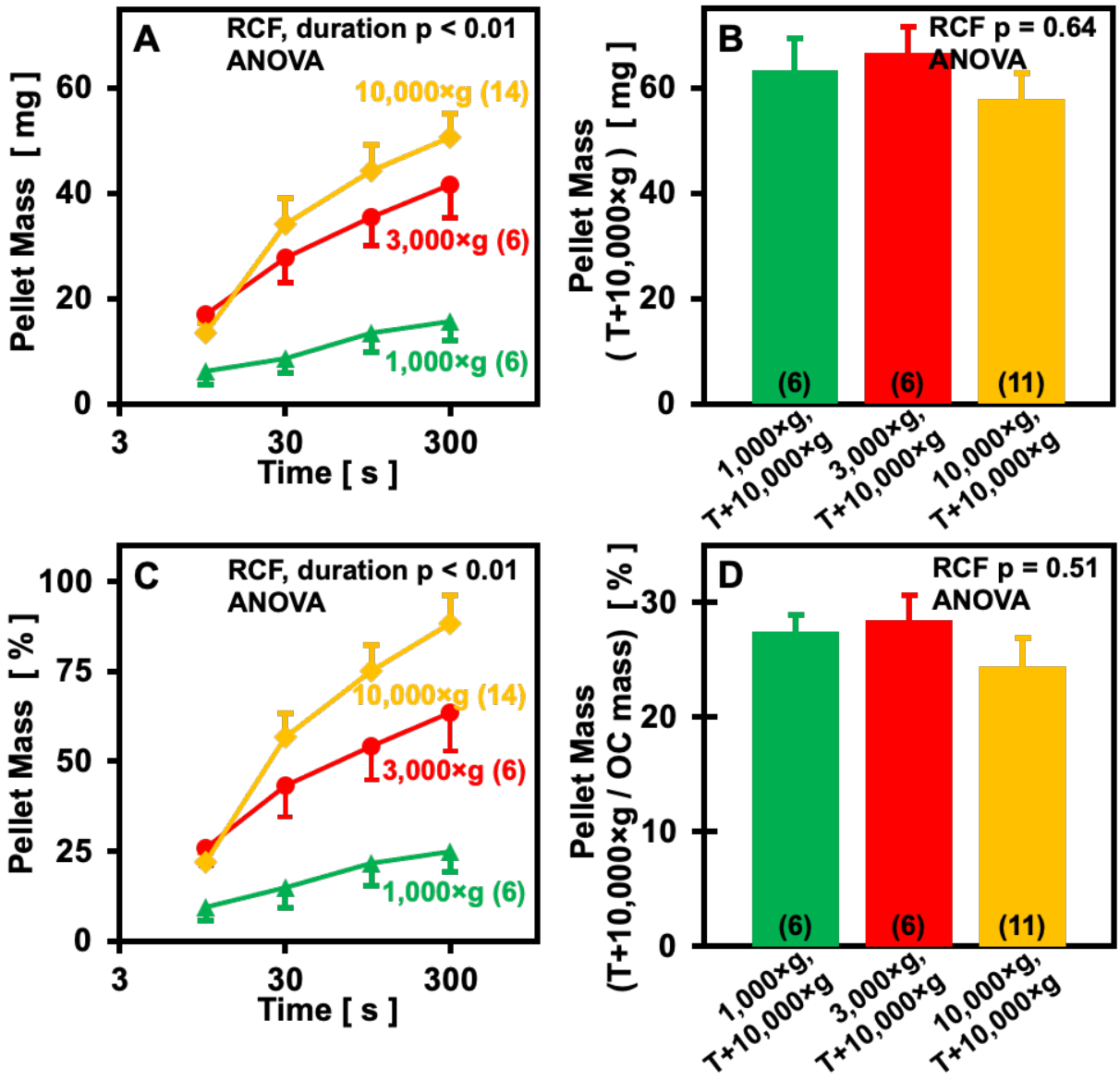

Figure 2.4. Effects of centrifugation RCF, duration, and trypsin treatment on indices of marrow removal from TKR-OCs. Effects of centrifugation duration (10, 30, 100, 300 s), RCF (1,000, 3,000, 10,000×g), and trypsin treatment before 10,000×g RCF (T+10,000×g). Pellet mass (**A**) after initial centrifugation, (**B**) after T+10,000×g, (**C**) from **A** relative to that from **B**, (**D**) Pellet mass after T+10,000×g relative to initial OC mass. Mean±SE. n=6-14.

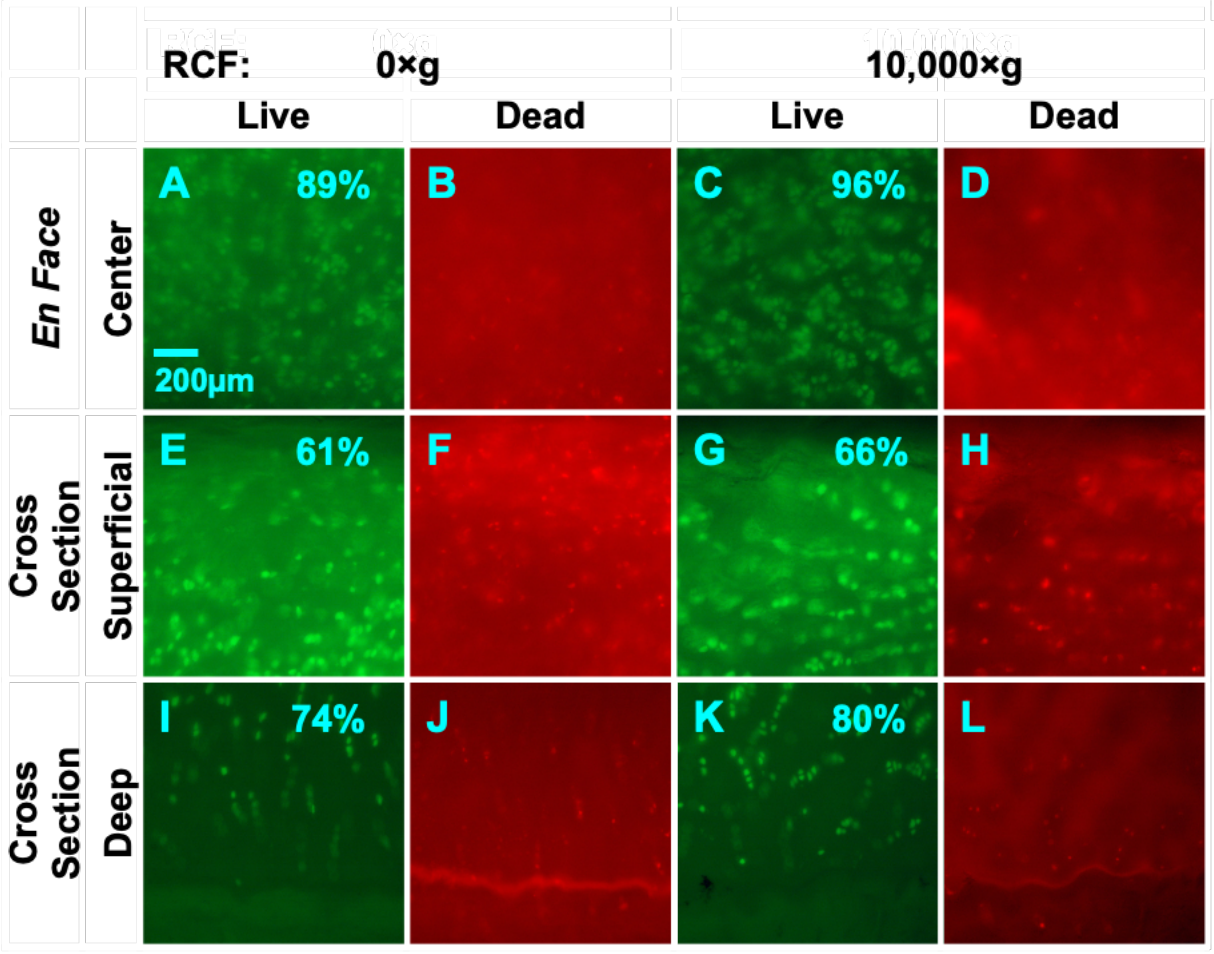

Figure 2.5. Effect of centrifugation on Live/Dead™ staining of TKR-OCs. (**A,C,E,G,I,K**) Live and (**B,D,F,H,J,L**) Dead images of articular cartilage of OCs (**A-B,E-F,I-J**) without and (**C-D,G-H,K-L**) after centrifugation at 10,000×g for 300s. (**A-D**) *En face* images, from the center of the sample. (**E-L**) Cross section images, at (**E-H**) superficial and (**I-L**) deep zones of the sample. Percentage values represent live / total cells.

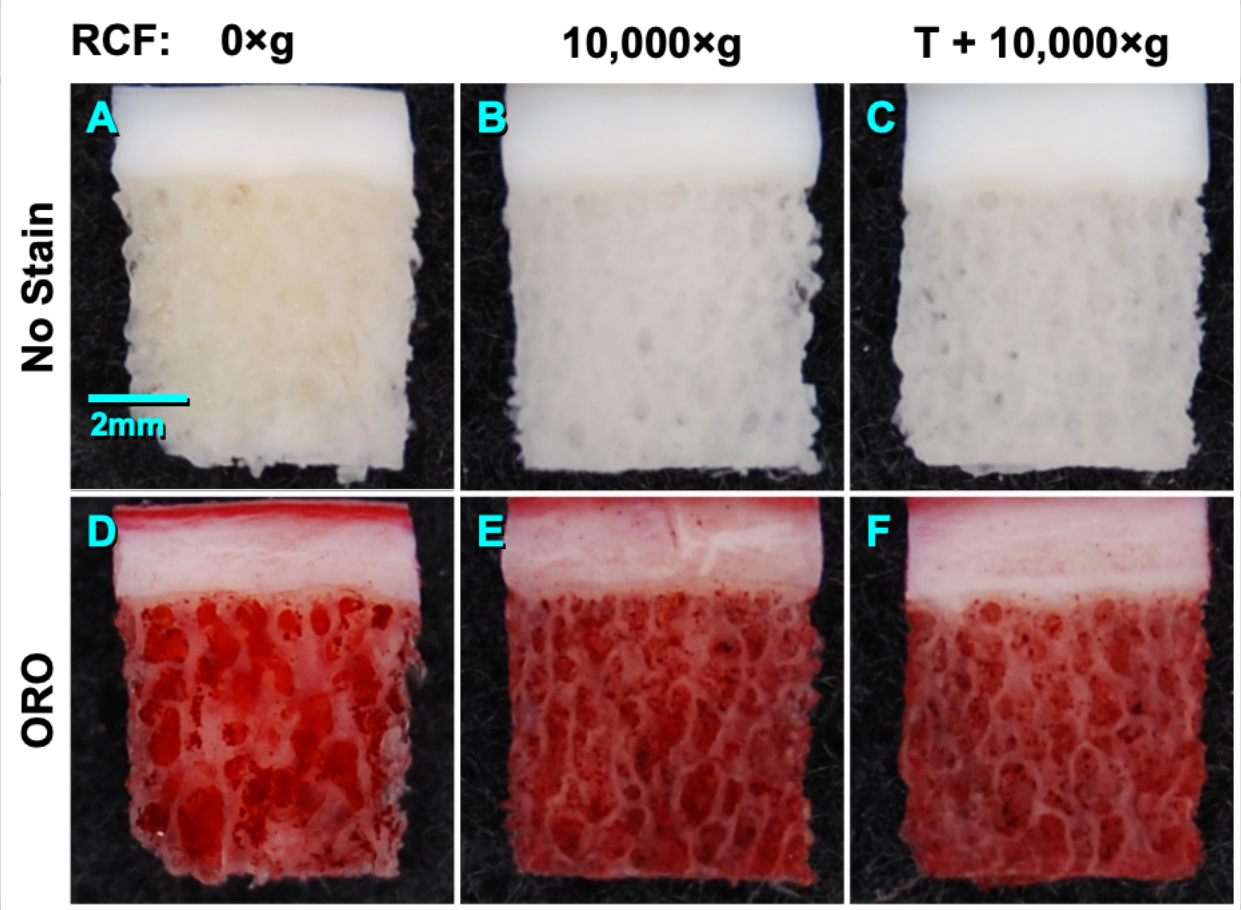

Figure 2.6. Effect of centrifugation on ORO staining of TKR-OCs. Gross images taken of bisected TKR-OCs (**A-C**) as prepared (no staining) and (**D-F**) after ORO staining, following (**A,D**) 0 or (**B,C,E,F**) 10,000×g centrifugation without (**B,E**) or with (**C,F**) prior trypsin treatment (T+10,000×g).

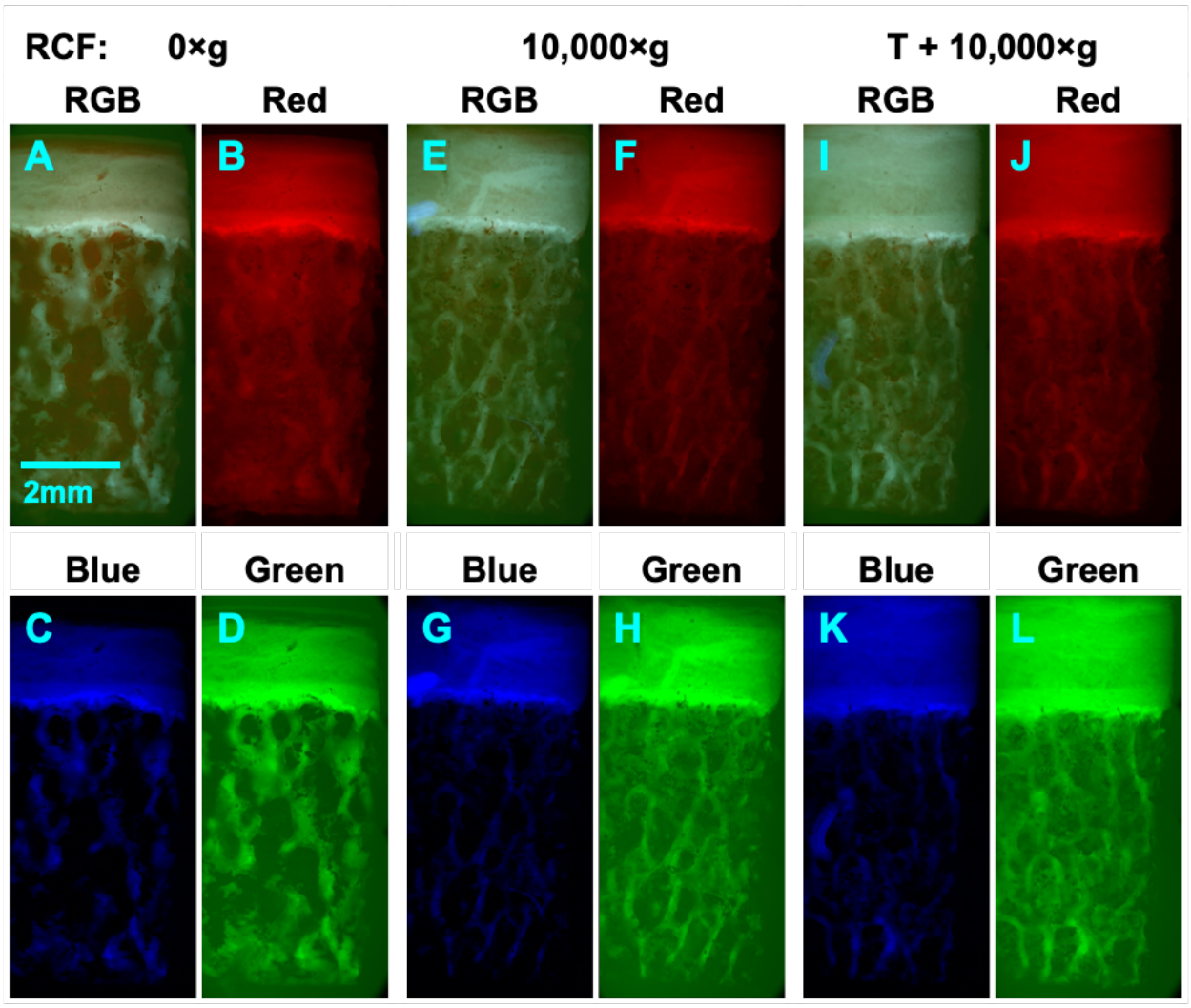

Figure 2.7. Representative fluorescence microscopy of effects of centrifugation on ORO staining of TKR-OCs. DAPI/FITC/Texas Red filtered microscopy of bisected OC surface after ORO staining with (**A-D**) 0, (**E-H**) 10,000×g, or (**I-L**) trypsin treatment before 10,000×g RCF (T+10,000×g) in (**A,E,I**) composite and (**B,F,J**) red (Texas Red), (**C,G,K**) blue (DAPI), and (**D,H,L**) green (FITC) signal.

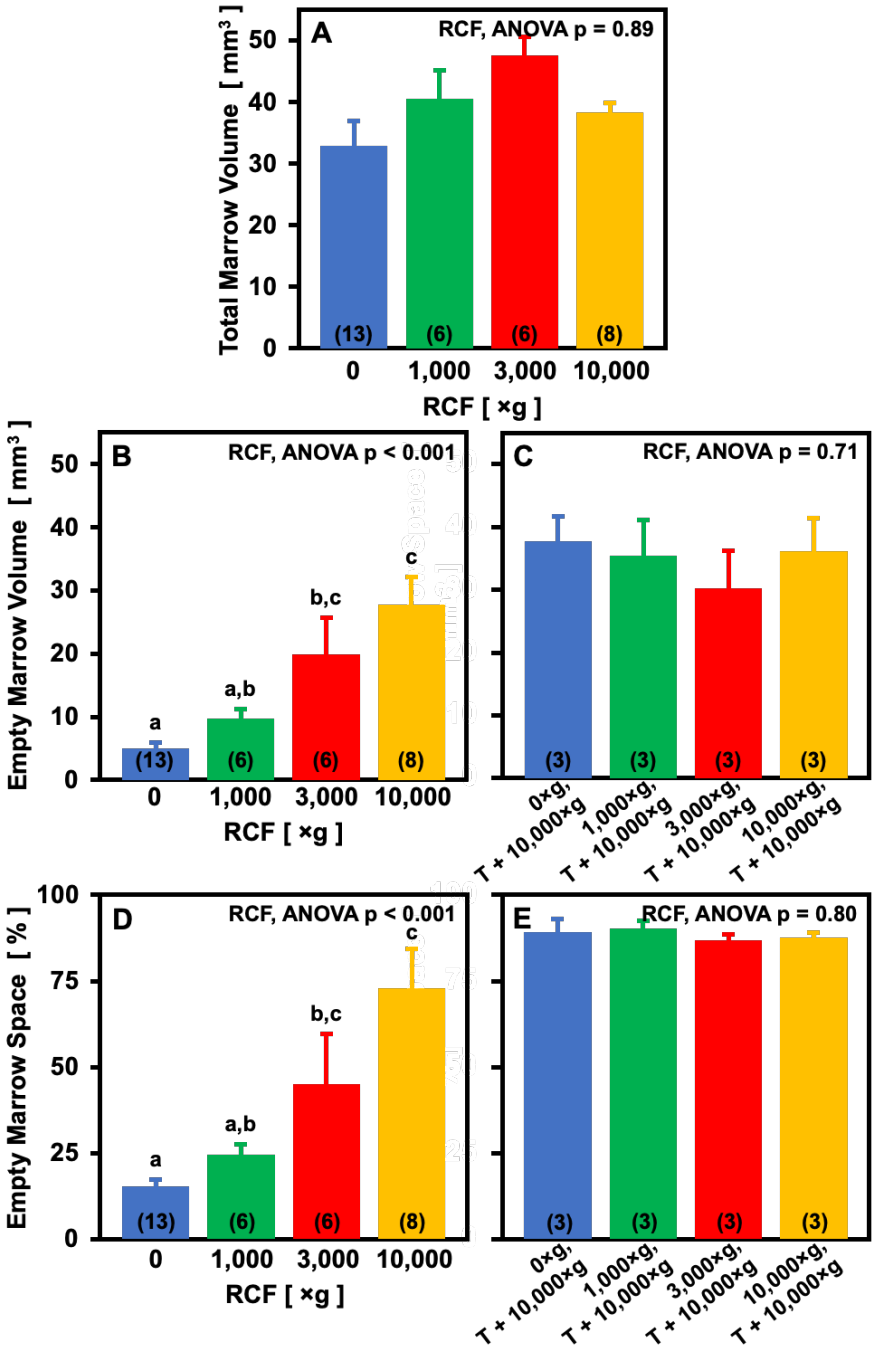

Figure 2.8. Effects of centrifugation RCF and trypsin pre-treatment on indices of marrow removal from TKR-OCs. Effects of RCF (0, 1,000, 3,000, 10,000×g), and trypsin treatment before 10,000×g RCF (T+10,000×g). (**A**) Total marrow volume. Empty marrow volume (**B**) after 300 s centrifugation and (**C**) after T + 10,000×g. Empty marrow space (**D**) from **B** relative to that from **A** and (**E**) from **C** relative to that from **A**. Mean±SE. n=3-13.

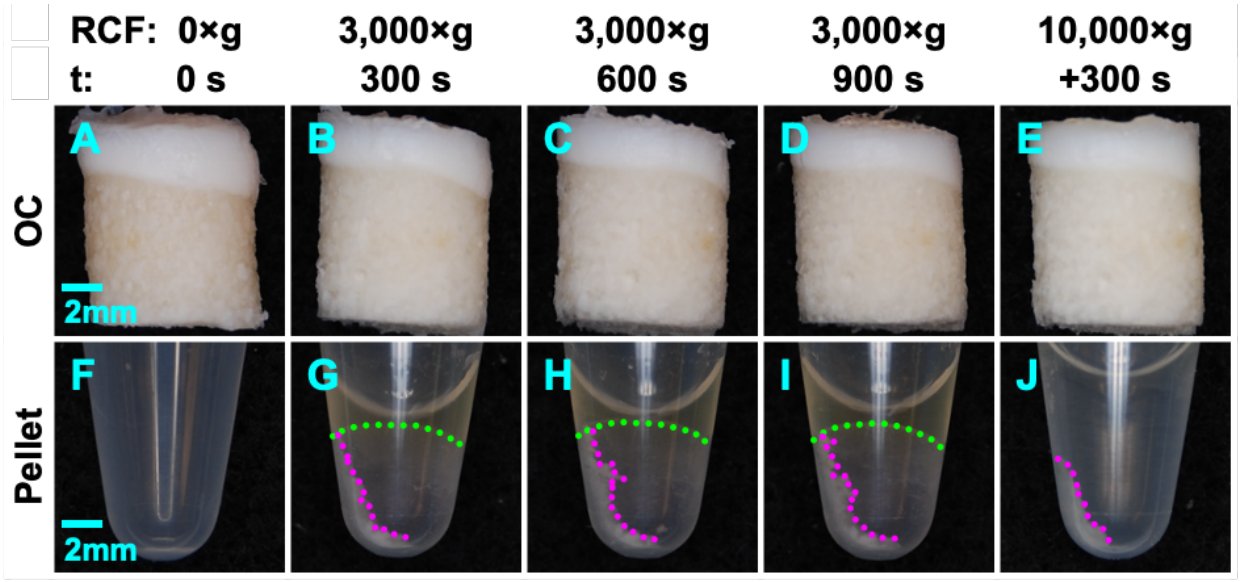

Figure 2.9. Representative gross images of OCA-OCs after centrifugation at different forces. Images of (**A-E**) gross core appearance after centrifugation for 0, 300, 600, or 900 s at varying RCF with (**F-J**) pellet at base of centrifuge tube.

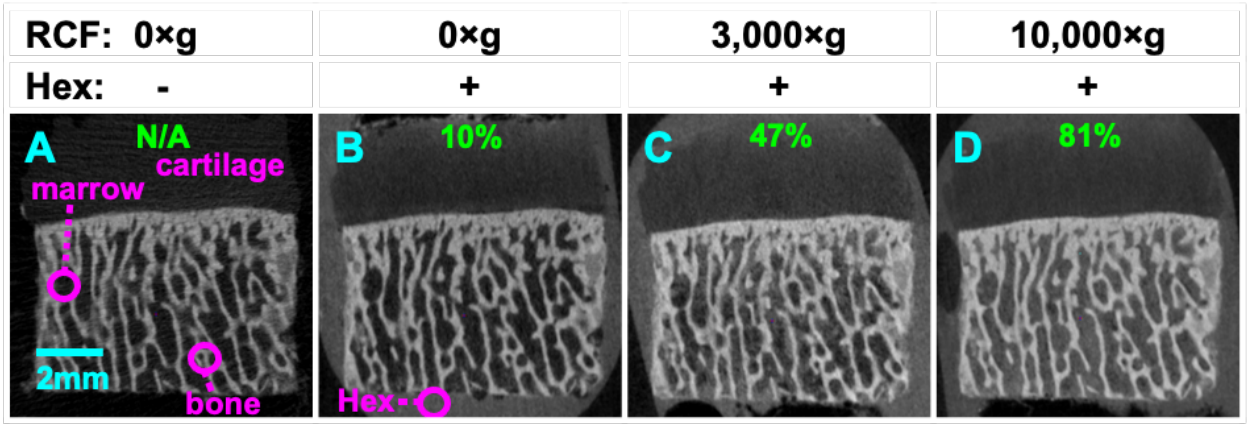

Figure 2.10. Representative µCT images (2D slices) of OCA-OCs pre- and post-centrifugation. Samples imaged (**A**) without and (**B-D**) with equilibration in Hex contrast (**A,B**) before and (**C,D**) after centrifugation for (**C**) 900 s at 3,000×g and (**D**) 300 s at 10,000×g. Image processing determination of empty marrow space indicated by percentage (green).

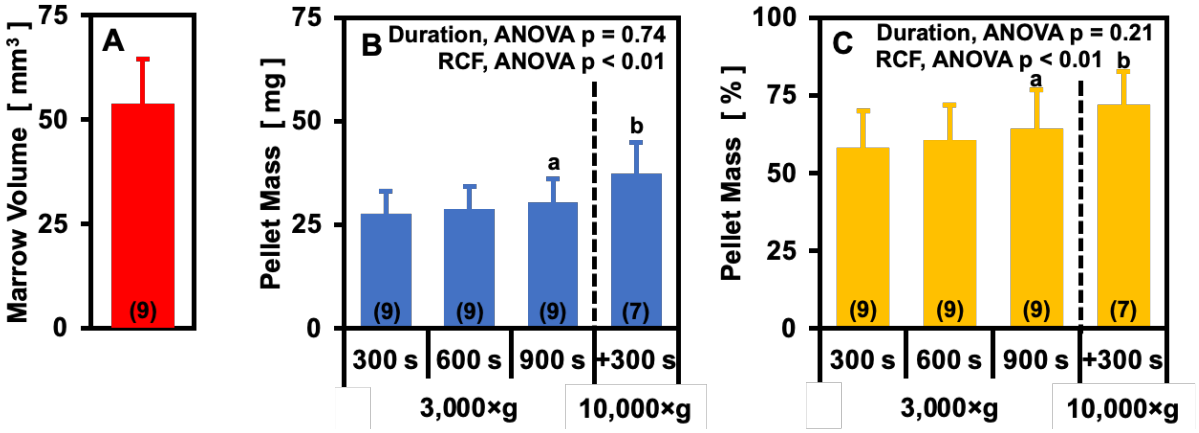

Figure 2.11. Effects of centrifugation RCF and duration on indices of marrow removal from OCA-OCs. Effects of centrifugation duration (300-900 s) and RCF (3,000, 10,000×g). (**A**) Marrow volume. Pellet mass (**B**) normalized by ROI volume and (**C**) from **B** relative to that from **A**. Mean±SE. n=7-9.

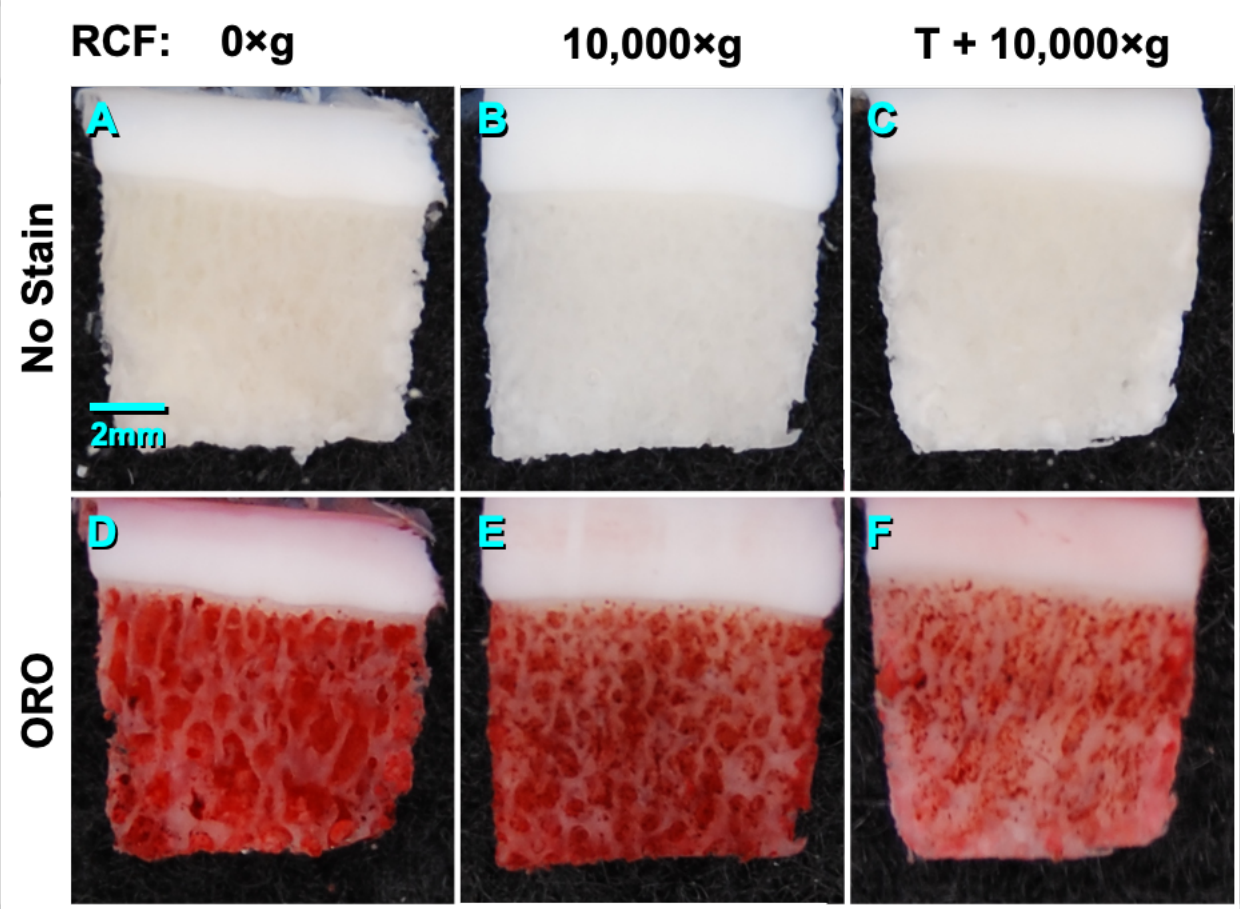

Figure 2.12. Effect of centrifugation on ORO staining of OCA-OCs. Gross images taken of bisected OCA-OCs (**A-C**) as prepared (no staining) and (**D-F**) after ORO staining, following (**A,D**) 0 or (**B,C,E,F**) 10,000×g centrifugation without (**B,E**) or with (**C,F**) prior trypsin treatment (T+10,000×g).

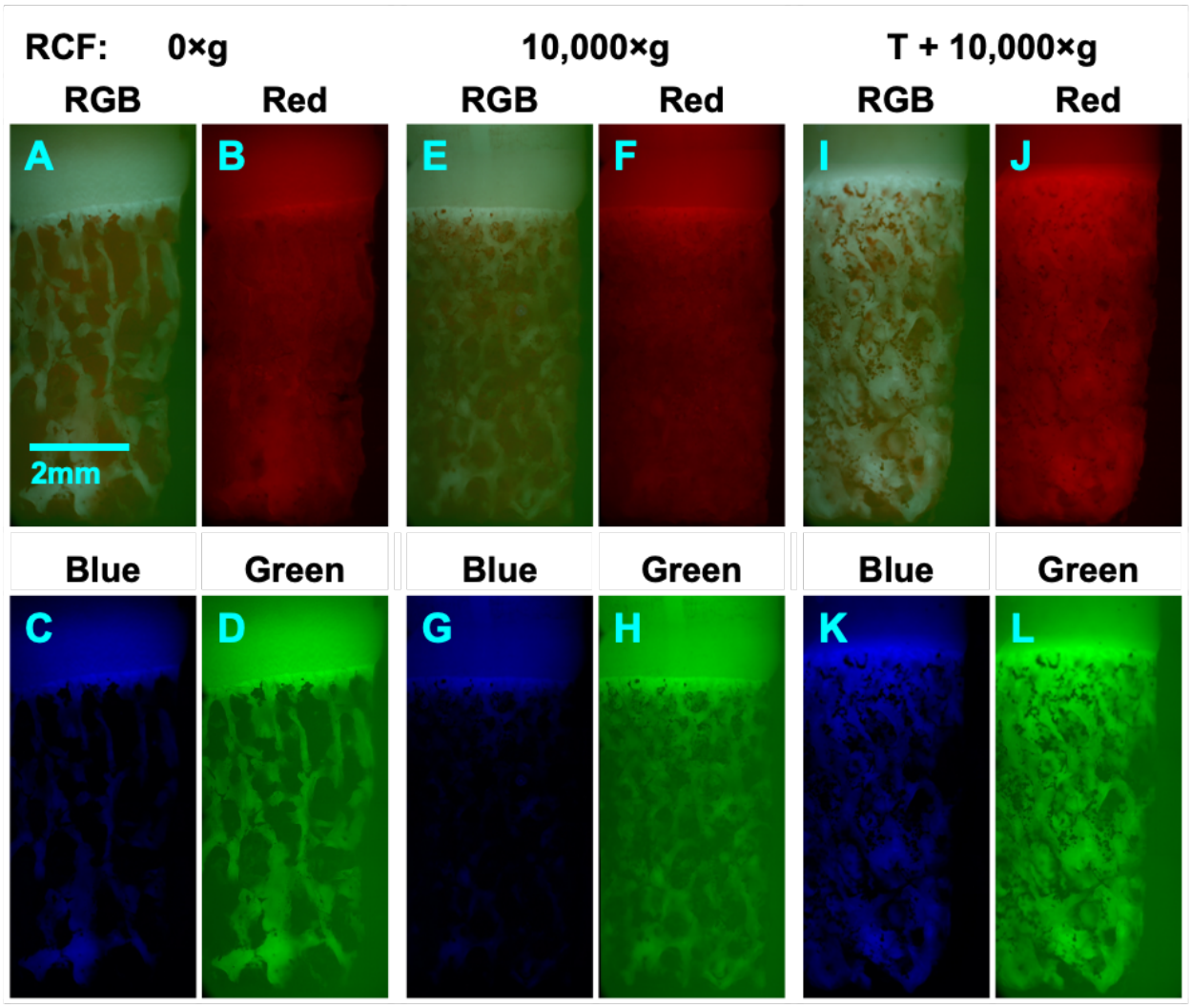

Figure 2.13. Representative fluorescence microscopy of effects of centrifugation on ORO staining of OCA-OCs. DAPI/FITC/Texas Red filtered microscopy of bisected OC surface after ORO staining with (**A-D**) 0, (**E-H**) 10,000×g, or (**I-L**) trypsin treatment before 10,000×g RCF (T+10,000×g) in (**A,E,I**) composite and (**B,F,J**) red (Texas Red), (**C,G,K**) blue (DAPI), and (**D,H,L**) green (FITC) signal.

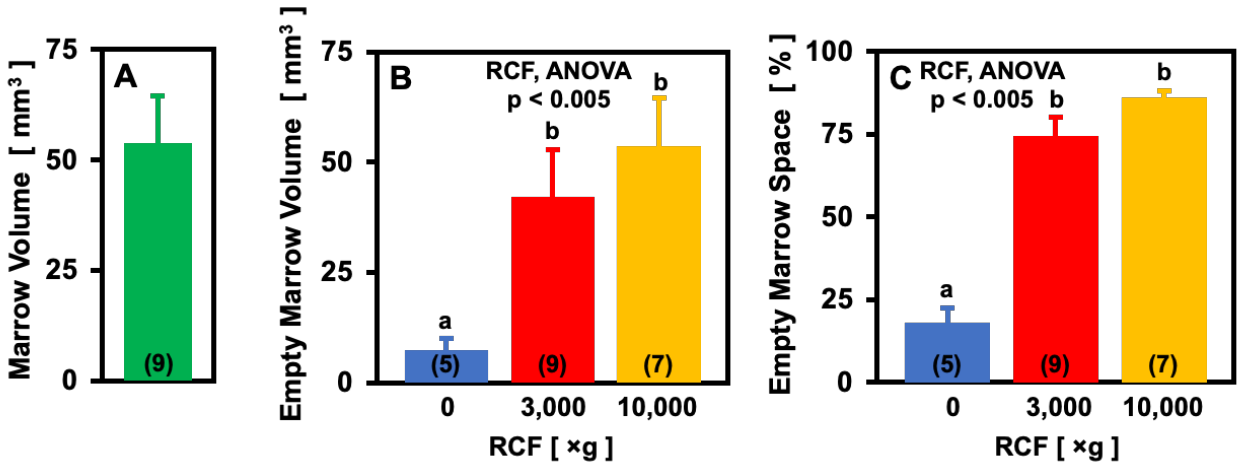

Figure 2.14. Effects of centrifugation RCF on indices of marrow removal from OCA-OCs. Effects of RCF (0, 3,000, 10,000×g). (**A**) Total marrow volume. (**B**) Empty marrow volume after 0, 900, or 1,200 s (900 +300 s) centrifugation. (**C**) Empty marrow space from **B** relative to that from **A**. Mean±SE. n=5-9.

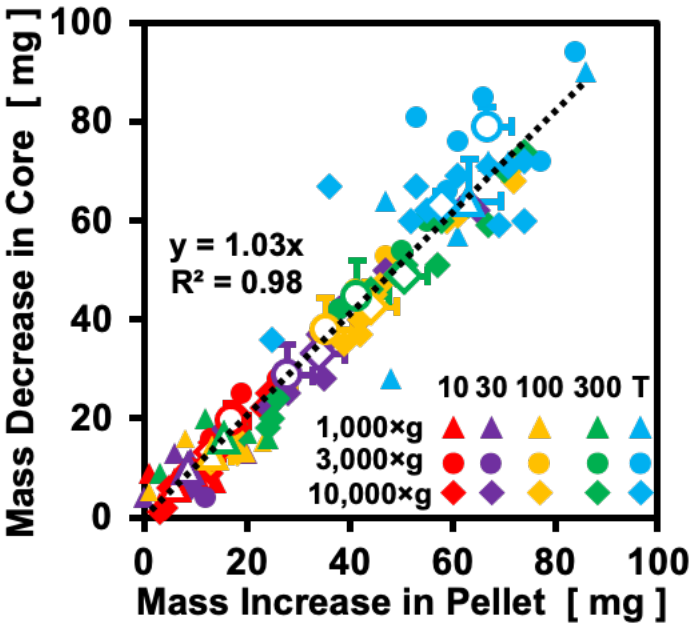

Figure 2.S1. Linear regression of mass difference in core vs. pellet mass. Mass decrease in core vs. increase in pellet with effects of centrifugation time (10, 30, 100, 300 s), RCF (1,000×g (▲), 3,000×g (●), 10,000×g (◆)), and trypsin (T) treatment on Human samples. Means (△,○, ◇) ± SE.

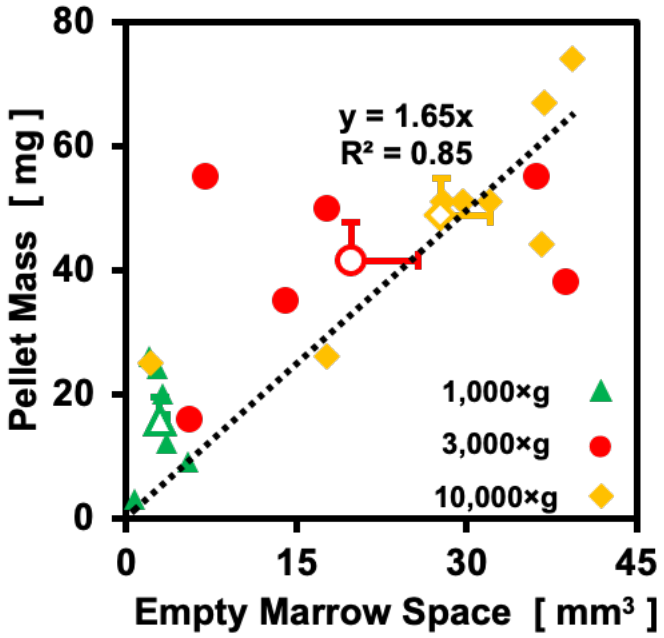

Figure 2.S2. Linear regression of empty marrow space vs. pellet mass. Empty marrow space (in VOI) vs. pellet mass with effects of RCF (▲1,000, ●3,000, ◆10,000) on TKR samples. Means (△,◯,◇) ± SE.

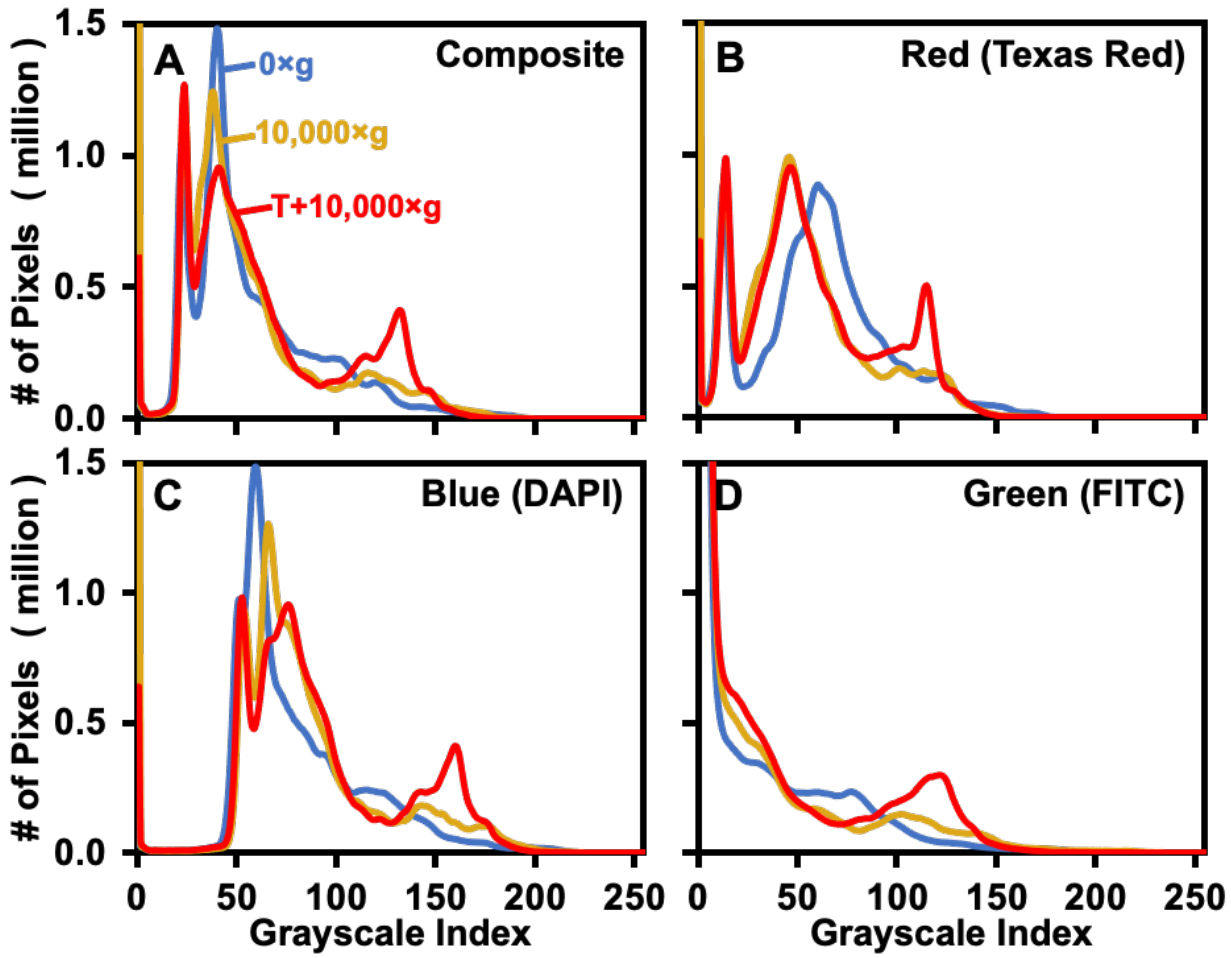

Figure 2.S3. Representative histograms from fluorescence microscopy images after ORO staining of TKR-OCs. Histograms from (**A**) composite and (**B**) red (Texas Red), (**C**) blue (DAPI), and (**D**) green (FITC) signal for 0 (blue), 10,000×g (yellow), or trypsin treatment before 10,000×g RCF (T+10,000×g, red) OCs.

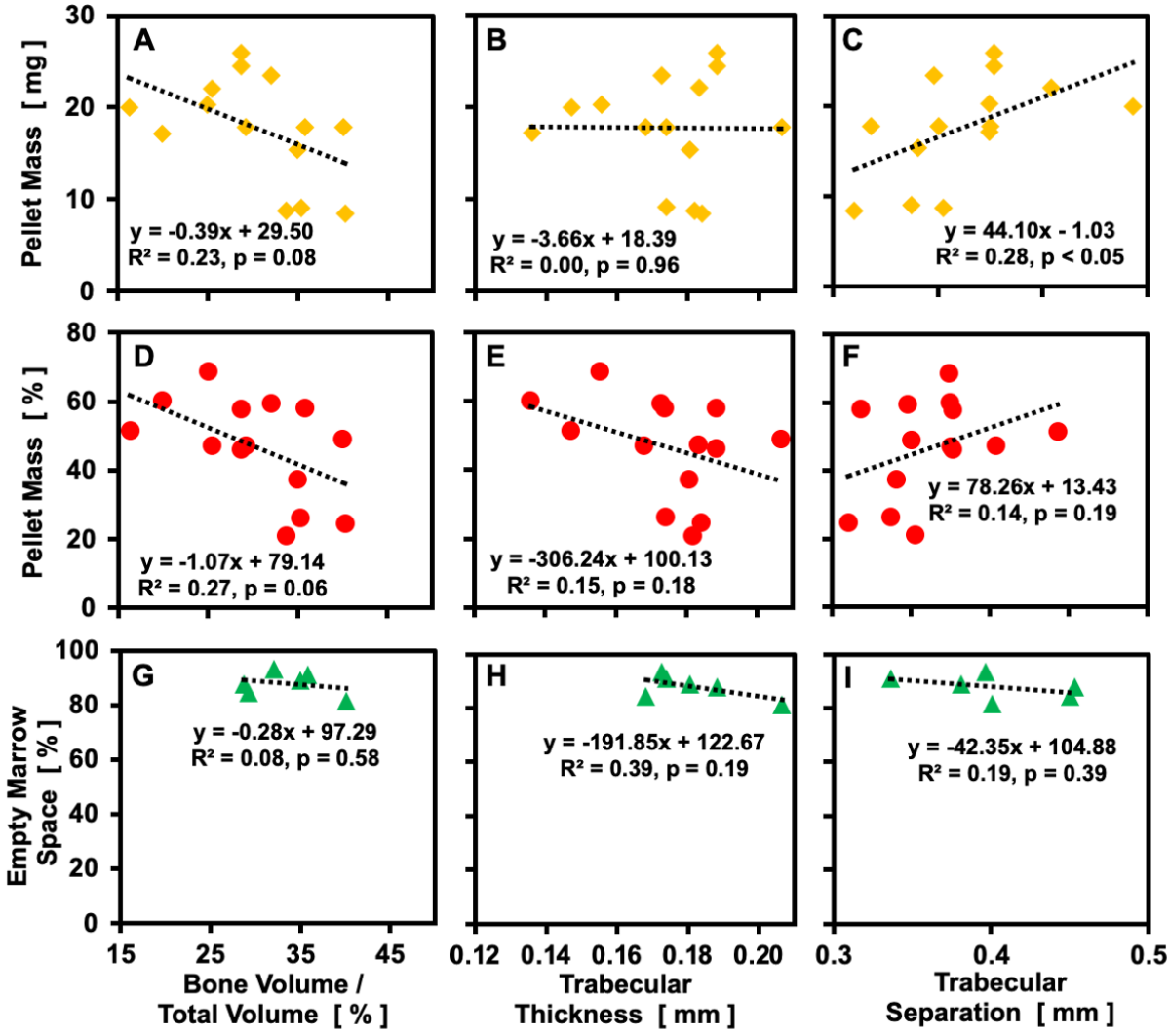

Figure 2.S4. Linear regression of bone morphometry vs. cleansing parameters on TKR-OCs without outliers. Bone morphometry parameters (**A,D,G**) bone volume relative to total volume, (**B,E,H**) trabecular thickness, and (**C,F,I**) trabecular separation vs. cleansing parameters (**A-C**) pellet mass, (**D-F**) pellet mass relative to T+10,000×g pellet mass, and (**G-I**) empty marrow space on TKR samples.

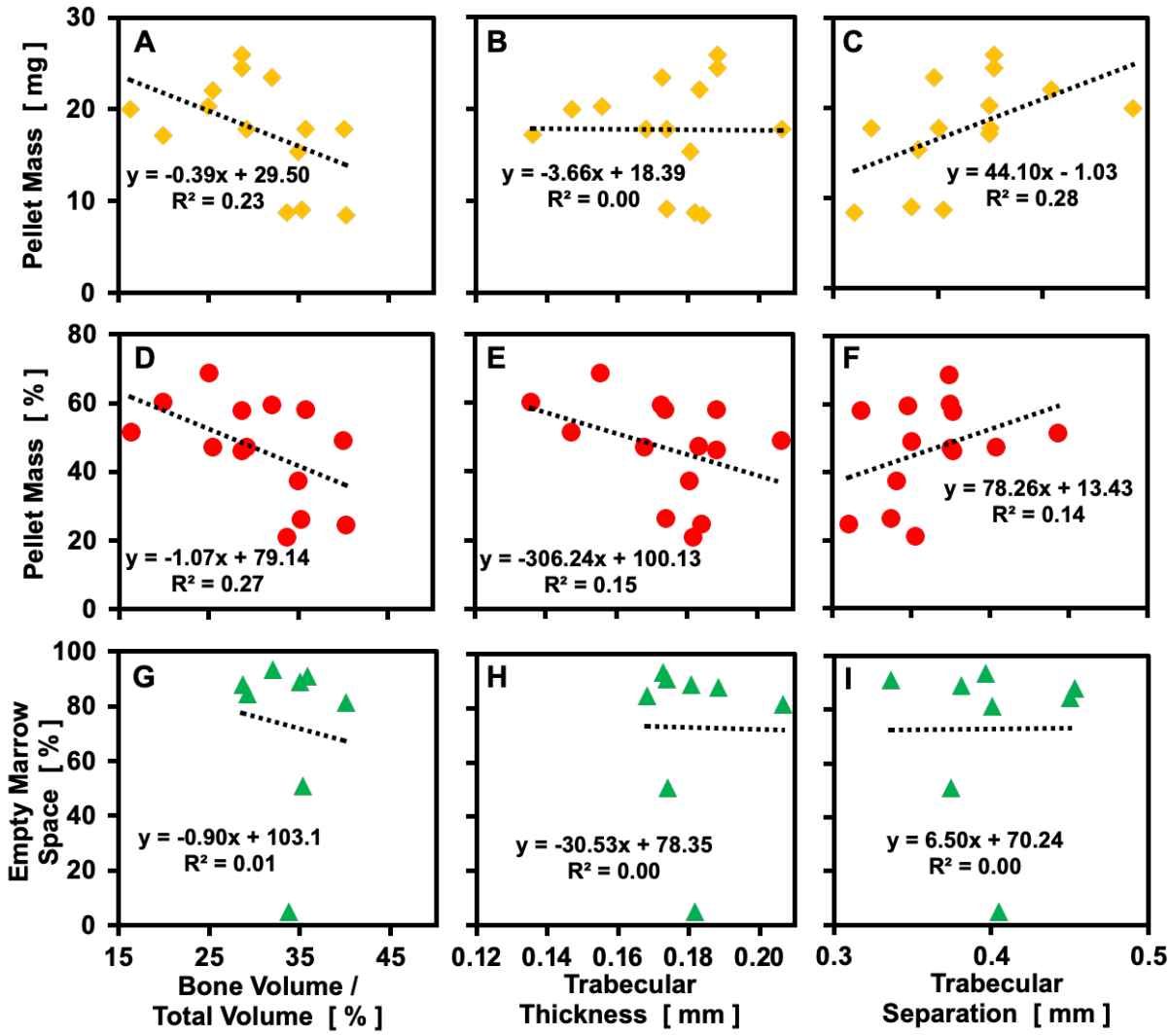

Figure 2.S5. Linear regression of bone morphometry vs. cleansing parameters on TKR-OCs with outliers. Bone morphometry parameters (**A,D,G**) bone volume relative to total volume, (**B,E,H**) trabecular thickness, and (**C,F,I**) trabecular separation vs. cleansing parameters (**A-C**) pellet mass, (**D-F**) pellet mass relative to T+10,000×g pellet mass, and (**G-I**) empty marrow space on TKR samples.

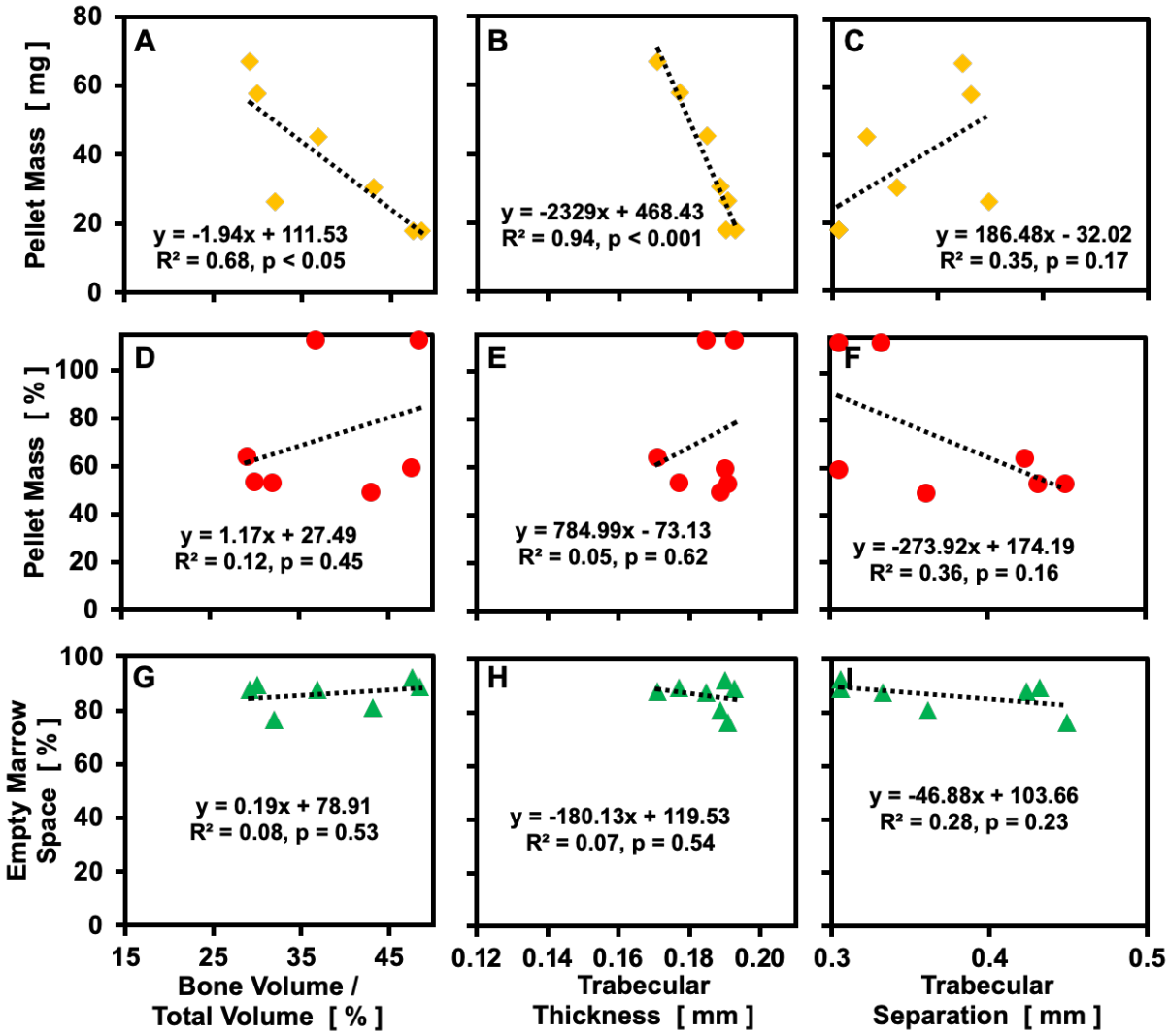

Figure 2.S6. Linear regression of bone morphometry vs. cleansing parameters on OCA-OCs. Bone morphometry parameters (**A,D,G**) bone volume relative to total volume, (**B,E,H**) trabecular thickness, and (**C,F,I**) trabecular separation vs. cleansing parameters (**A-C**) pellet mass, (**D-F**) pellet mass relative to T+10,000×g pellet mass, and (**G-I**) empty marrow space on OCA samples.

2.7 TABLES

Table 2.1. Trabecular bone morphometry for TKR-OCs from normal post-mortem femoral condyles of adult human total knee arthroplasty (TKR) and osteochondral allograft (OCA). Bone parameters from OCs prior to centrifugation at 0, 1,000, 3,000, or 10,000×g. Mean +/- SE. n = 6-14.

Tissue Type	RCF [×g]	Total VOI volume	Bone volume	Bone volume fraction	Trabecular thickness	Trabecular separation	n	Donors	Age [yrs]	M/F
		TV	BV	BV/TV	Tb.Th	Tb.Sp				
		mm^3	mm^3	%	mm	mm				
TKR	0	55.1±6.6	13.9±1.8	25.7±2.1	0.162±0.005	0.465±0.029	13	13	71±3	3/10
TKR	1,000	65.9±5.4	18.6±1.9	28.6±2.6	0.167±0.006	0.432±0.031	6	5	72±2	0/5
TKR	3,000	71.3±6.1	18.4±3.3	25.3±3.0	0.160±0.012	0.444±0.015	6	4	72±5	3/1
TKR	10,000	63.8±3.1	20.0±1.9	30.4±1.9	0.174±0.005	0.426±0.018	14	10	71±3	4/6
TKR	**Total**	**62.4±2.8**	**17.5±1.1**	**27.8±1.2**	**0.167±0.003**	**0.442±0.013**	**39**	**16**	**71±3**	**4/12**
OCA	**Total**	**104.3±16.0**	**37.9±4.6**	**38.3±2.6**	**0.188±0.006**	**0.371±0.019**	**9**	**4**	**20±1**	**4/0**

Table 2.S1. Table of experimental groups. OCs from normal post-mortem femoral condyles of adult human total knee arthroplasty (TKR). Each sample subjected to Radial Centrifugal Force (RCF) for a total of 0, 10, 30, 100, or 300 s, and an additional 300 s at 10,000×g post-trypsin.

Grp	***Type***	***RCF [×g]***	***RCF* [×g]***	***n***
1	TKR	0	10,000	6
2	TKR	1,000	10,000	6
3	TKR	3,000	10,000	6
4	TKR	10,000	10,000	14

Table 2.S2. Table of experimental groups. OCs from normal post-mortem femoral condyles of osteochondral allografts (OCA). Each sample subjected to Radial Centrifugal Force (RCF) for a total of 0, 300, 600, 900, and 1,200 s (900 +300 s).

Grp	***Type***	***RCF [×g]***	***t =***	***n***
1	OCA	0	0 s	9
2	OCA	3,000	300, 600, 900 s	9
3	OCA	10,000	300 s	9

2.8 REFERENCES

1. Methods of Cell Separation: Elsevier; 1988.

2. Ahmed TA, Hincke MT: Strategies for articular cartilage lesion repair and functional restoration. *Tissue Eng Part B Rev* 16:305-29, 2010.

3. Aubin PP, Cheah HK, Davis AM, Gross AE: Long-term followup of fresh femoral osteochondral allografts for posttraumatic knee defects. *Clin Orthop Relat Res* 391 Suppl:318-27, 2001.

4. Bouxsein ML, Boyd SK, Christiansen BA, Guldberg RE, Jepsen KJ, Muller R: Guidelines for assessment of bone microstructure in rodents using micro-computed tomography. *J Bone Miner Res* 25:1468-86, 2010.

5. Brown K, Schluter S, Sheppard A, Wildenschild D: On the challenges of measuring interfacial characteristics of three-phase fluid flow with x-ray microtomography. *J Microsc* 253:171-82, 2014.

6. Bugbee W, Cavallo M, Giannini S: Osteochondral allograft transplantation in the knee. *J Knee Surg* 25:109-16, 2012.

7. Bugbee WD, Convery FR: Osteochondral allograft transplantation. *Clin Sports Med* 18:67-75, 1999.

8. Bugbee WD, Khanna G, Cavallo M, McCauley JC, Görtz S, Brage ME: Bipolar fresh osteochondral allografting of the tibiotalar joint. *J Bone Joint Surg Am* 95:426-32, 2013.

9. Bugbee WD, Pallante-Kichura AL, Görtz S, Amiel D, Sah R: Osteochondral allograft transplantation in cartilage repair: Graft storage paradigm, translational models, and clinical applications. *J Orthop Res* 34:31-8, 2016.

10. Cook JL, Stannard JP, Stoker AM, Bozynski CC, Kuroki K, Cook CR, Pfeiffer FM: Importance of donor chondrocyte viability for osteochondral allografts. *Am J Sports Med* 44:1260-8, 2016.

11. Cook JL, Stoker AM, Stannard JP, Kuroki K, Cook CR, Pfeiffer FM, Bozynski C, Hung CT: A novel system improves preservation of osteochondral allografts. *Clin Orthop Relat Res* 472:3404-14, 2014.

12. Demontiero O, Li W, Thembani E, Duque G: Validation of noninvasive quantification of bone marrow fat volume with microCT in aging rats. *Exp Gerontol* 46:435-40, 2011.

13. Dempster DW, Compston JE, Drezner MK, Glorieux FH, Kanis JA, Malluche H, Meunier PJ, Ott SM, Recker RR, Parfitt AM: Standardized nomenclature, symbols, and units for bone

histomorphometry: a 2012 update of the report of the ASBMR Histomorphometry Nomenclature Committee. *J Bone Miner Res* 28:2-17, 2013.

14. Desjardins MR, Hurtig MB, Palmer NC: Incorporation of fresh and cryopreserved bone in osteochondral autografts in the horse. *Vet Surg* 20:446-52, 1991.

15. Eagle MJ, Man J, Rooney P, Hogg P, Kearney JN: Assessment of an improved bone washing protocol for deceased donor human bone. *Cell Tissue Bank* 16:83-90, 2015.

16. Eagle MJ, Man J, Rooney P, Kearney JN: Comparison of bone marrow component removal from processed femoral head bone from living and deceased donors: presence of geodes in living donor bone can prevent maximum removal of marrow components. *Cell Tissue Bank* 19:727-32, 2018.

17. Eagle MJ, Man J, Rooney P, McQuillan TA, Galea G, Kearney JN: Assessment of a closed wash system developed for processing living donor femoral heads. *Cell Tissue Bank* 18:547-54, 2017.

18. Enneking WF, Mindell ER: Observations on massive retrieved human allografts. *J Bone Joint Surg Am* 73-A:1123-42, 1991.

19. Garrett JC: Fresh osteochondral allografts for treatment of articular defects in osteochondritis dissecans of the lateral femoral condyle in adults. *Clin Orthop Relat Res* 303:33-7, 1994.

20. Glenn RE, Jr., McCarty EC, Potter HG, Juliao SF, Gordon JD, Spindler KP: Comparison of fresh osteochondral autografts and allografts: a canine model. *Am J Sports Med* 34:1084-93, 2006.

21. Goldberg VM: Natural history of autografts and allografts. In: *Bone implant grafting,* ed. by Springer, London, 1992, 9-12.

22. Gortz S, Bugbee WD: Allografts in articular cartilage repair. *Instructional Course Lectures* 56:469-80, 2007.

23. Görtz S, Tabbaa SM, Jones DG, Polousky JD, Crawford DC, Bugbee WD, Cole BJ, Farr J, Fleischli JE, Getgood A, Gomoll AH, Gross AE, Krych AJ, Lattermann C, Mandelbaum BR, Mandt PR, Mirzayan R, Mologne TS, Provencher MT, Rodeo SA, Safir O, Strauss ED, Wahl CJ, Williams RJ, Yanke AB: Metrics of OsteoChondral Allografts (MOCA) group consensus statements on the use of viable osteochondral allograft. *Orthop J Sports Med* 9:2325967120983604, 2021.

24. Gross AE, Shasha N, Aubin P: Long-term followup of the use of fresh osteochondral allografts for posttraumatic knee defects. *Clin Orthop Relat Res* 435:79-87, 2005.

25. Gurkan UA, Akkus O: The mechanical environment of bone marrow: a review. *Ann Biomed Eng* 36:1978-91, 2008.

26. Haimi S, Wahlman M, Mannila M, Virtanen V, Hirn M: Pulse-lavage washing is an effective method for defatting of morselized allograft bone in the operating theater. *Acta Orthop* 79:94-7, 2008.

27. Kalteis T, Pforringer D, Herold T, Handel M, Renkawitz T, Plitz W: An experimental comparison of different devices for pulsatile high-pressure lavage and their relevance to cement intrusion into cancellous bone. *Arch Orthop Trauma Surg* 127:873-7, 2007.

28. LaPrade RF, Botker J, Herzog M, Agel J: Refrigerated osteoarticular allografts to treat articular cartilage defects of the femoral condyles. A prospective outcomes study. *J Bone Joint Surg Am* 91:805-11, 2009.

29. Lewandrowski KU, Rebmann V, Päßler M, Schollmeier G, Ekkernkamp A, Grosse-Wilde H, Tomford WW: Immune response to perforated and partially demineralized bone allografts. *J Orthop Sci* 6:545–55, 2001.

30. Li W, You L, Schaffler MB, Wang L: The dependency of solute diffusion on molecular weight and shape in intact bone. *Bone* 45:1017-23, 2009.

31. Li X, Anton N, Zuber G, Vandamme T: Contrast agents for preclinical targeted X-ray imaging. *Adv Drug Deliv Rev* 76:116-33, 2014.

32. Lomas R, Drummond O, Kearney JN: Processing of whole femoral head allografts: a method for improving clinical efficacy and safety. *Cell Tissue Bank* 1:193-200, 2000.

33. Luedtke-Hoffmann KA, Schafer DS: Pulsed lavage in wound cleansing. *Phys Ther* 80:292-300, 2000.

34. Marom N, Bugbee W, Williams RJ: Osteochondral grafts failures. *Oper Tech Sports Med*, 2019.

35. McCulloch PC, Kang RW, Sobhy MH, Hayden JK, Cole BJ: Prospective evaluation of prolonged fresh osteochondral allograft transplantation of the femoral condyle: minimum 2-year follow-up. *Am J Sports Med* 35:411-20, 2007.

36. Meyer MA, McCarthy MA, Gitelis ME, Poland SG, Urita A, Chubinskaya S, Yanke AB, Cole BJ: Effectiveness of lavage techniques in removing immunogenic elements from osteochondral allografts. *Cartilage* 8:369-73, 2017.

37. Oakeshott RD, Farine I, Pritzker KPH, Langer F, Gross AE: A clinical and histologic analysis of failed fresh osteochondral allografts. *Clin Orthop Relat Res* 233:283-94, 1988.

38. Pallante AL, Chen AC, Ball ST, Amiel D, Masuda K, Sah RL, Bugbee WD: The in vivo performance of osteochondral allografts in the goat is diminished with extended storage and decreased cartilage cellularity. *Am J Sports Med* 40:1814-23, 2012.

39. Pallante AL, Gortz S, Chen AC, Healey RM, Chase DC, Ball ST, Amiel D, Sah RL, Bugbee WD: Treatment of articular cartilage defects in the goat with frozen versus fresh osteochondral allografts: effects on cartilage stiffness, zonal composition, and structure at six months. *J Bone Joint Surg Am* 94:1984-95, 2012.

40. Pallante-Kichura AL, Cory E, Bugbee WD, Sah RL: Bone cysts after osteochondral allograft repair of cartilage defects in goats suggest abnormal interaction between subchondral bone and overlying synovial joint tissues. *Bone* 57:259–68, 2013.

41. Palmer AW, Guldberg RE, Levenston ME: Analysis of cartilage matrix fixed charge density and three-dimensional morphology via contrast-enhanced microcomputed tomography. *Proc Natl Acad Sci U S A* 103:19255-60, 2006.

42. Ranawat AS, Vidal AF, Chen CT, Zelken JA, Turner AS, Williams RJ, 3rd: Material properties of fresh cold-stored allografts for osteochondral defects at 1 year. *Clin Orthop Relat Res* 466:1826-36, 2008.

43. Rodeheaver GT, Pettry D, Thacker JG, Edgerton MT, Edlich RF: Wound cleansing by high pressure irrigation. *Surg Gynecol Obstet* 141:357-62, 1975.

44. Rodrigo JJ, Thompson E, Travis C: Deep-freezing versus 4° preservation of avascular osteocartilaginous shell allografts in rats. *Clin Orthop Relat Res* 218:268-75, 1987.

45. Sadr KN, Pulido PA, McCauley JC, Bugbee WD: Osteochondral allograft transplantation in patients with osteochondritis dissecans of the knee. *Am J Sports Med* 44:2870-5, 2016.

46. Sirlin CB, Brossmann J, Boutin RD, Pathria MN, Convery FR, Bugbee W, Deutsch R, Lebeck LK, Resnick D: Shell osteochondral allografts of the knee: comparison of mr imaging findings and immunologic responses. *Radiology* 219:35-43, 2001.

47. Smith CA, Richardson SM, Eagle MJ, Rooney P, Board T, Hoyland JA: The use of a novel bone allograft wash process to generate a biocompatible, mechanically stable and osteoinductive biological scaffold for use in bone tissue engineering. *J Tissue Eng Regen Med* 9:595-604, 2015.

48. Stevenson S: The immune response to osteochondral allografts in dogs. *J Bone Joint Surg Am* 69-A:573-82, 1987.

49. Strong DM, Friedlaender GE, Tomford WW, Springfield DS, Shives TC, Burchardt H, Enneking WF, Mankin HJ: Immunologic responses in human recipients of osseous and osteochondral allografts. *Clin Orthop Relat Res* 326:107-14, 1996.

50. Sun Y, Jiang W, Cory E, Caffrey JP, Hsu FH, Chen AC, Wang J, Sah RL, Bugbee WD: Pulsed lavage cleaning of osteochondral grafts depends on lavage duration, flow intensity, and graft storage condition. *PLoS One* 12:e0176934, 2017.

51. VandeVord PJ, Nasser S, Wooley PH: Immunological responses to bone soluble proteins in recipients of bone allografts. *J Orthop Res* 23:1059-64, 2005.

52. Williams RJ, 3rd, Ranawat AS, Potter HG, Carter T, Warren RF: Fresh stored allografts for the treatment of osteochondral defects of the knee. *J Bone Joint Surg Am* 89:718-26, 2007.

CHAPTER 3. CONCLUSIONS

3.1 Summary of Findings

The aims of this work were to determine the effectiveness of centrifugation in cleansing marrow space on osteochondral cores from both total knee remnant and osteochondral allograft sources. For TKR-OCs and OCA-OCs, the (A) effectiveness was evaluated for different (i) centrifugation intensities and (ii) durations, (B) histological representation of marrow cell elements (blood, hematopoietic, and adipose cells) present, and (C) maintenance of chondrocyte viability post-centrifugation, and pre- and post-centrifugation. To address these aims, novel approaches were taken. In summary, the novel methodologies were:

1. The development of a tidy centrifugation method, using a common desktop centrifuge and sample holder, for use in removing marrow from OCAs.
2. The measurement of centrifuged pellet mass for sample-specific quantitation of removed marrow.
3. The use of trypsin treatment and additional centrifugation for a biochemical positive control for the mass measure of OCA cleansing.

The major findings related to the scientific objectives were:

1. A dose-dependence of centrifuge force and duration for OC cleansing.
    a. Marrow was gradually released from OCs with longer durations of centrifugation for all RCF, though the marrow release reached a plateau after ~300 s of centrifugation. The duration of centrifugation could potentially allow for modulation of marrow release.

b. The marrow release from both TKR and OCA-OCs was higher with high RCF, allowing for a tailored approach in future OCA cleansing.

2. Cleansing of TKR and OCA-OCs by centrifugation at high RCF (10,000×g) achieved moderately high marrow removal after 300 s of centrifugation (73±11 % in TKR-OCs and 86±2 % in OCA-OCs), which is comparable to the 65 and 78 % marrow removed via standard pulsed saline lavage and combination pulsed saline and CO2 lavage, respectively.[7]
3. High chondrocyte viability was maintained with centrifugation at high RCF (10,000×g).
    a. In *en face* images beyond the first ~200 μm from the cut edge, both live and dead cells were prominent, with 99±1 and 90±1 % cell viability (Live / Total cells) in 0 and 10,000×g groups, respectively.
    b. Live and dead cells were prominent beyond the edge of the cartilage, with 93±2 and 90±3 % cell viability, in superficial and middle/deep zones, for both 0 and 10,000×g groups.
4. A relationship between bone morphometry and the release of marrow from OCs.
    a. BV/TV and trabecular thickness yielded more marrow release with larger bone volume and trabecular thickness, while marrow release was less with larger trabecular separation.
    b. Visually, horizontal bone struts were often observed below pockets of remaining marrow.

3.2 Discussion

The present work can be expanded in the future in a number of ways. The dose-dependence of centrifuge force and duration could be assessed for larger or thicker OC samples to determine

if the patterns of marrow removal remain similar across samples of all sizes. This work studied OCs with a 6 or 8 mm diameter and 5 mm subchondral bone height, but OCs with diameters of up to 35 mm diameter and subchondral bone heights ranging 3-10 mm (at the edge) are used clinically.[1,8] Pulsed lavage cleansing of OCAs, had marrow removal that started in the center of the sample base and progressed upward and towards the edges of the sample.[10] Cleansing by centrifugation had marrow cleansing that started at the sample base and progressed upwards. Once the trends in marrow removal are fully characterized for centrifugal cleansing, marrow removal can be tailored in both quantity and locally.

The use of trypsin as a method to loosen the marrow to achieve functional empty marrow space by centrifugation was effective. However, in measurement of the functional empty marrow space, since μCT has a finite voxel size and effective resolution, the image processing sequence will also effect the exact numbers. However, the correlation between pellet mass and empty marrow volume (**Fig. 2.S2**) indicate a linear relationship, though the relationship reflects in a slope of 1.65 due to the measurement of empty marrow volume within a defined VOI that is ~45 % less (total subchondral bone volume ~ 127 mm^3, VOI ~ 69 mm^3) than the full subchondral bone region (**Table 2.1**).

Since the marrow release from OCs was influenced by the bone morphometry parameters, future studies could investigate methods of releasing remaining marrow from OCs. For marrow to release from trabecular bone, channels must exist within the subchondral bone for which the marrow can escape. Visually, μCT after centrifugation showed pockets of retained marrow in OCs that were often above horizontal bone struts. Centrifugation in this and previous studies used sample setups that allowed for RCF to be along the vertical axis of an upright OCA sample, thus allowing for marrow to release along the same axis.[3,4,9] For a marrow pocket that is blocked by a

horizontal strut, the marrow may be better released by modifying the orientation of the sample. Thus, further studies can assess this modification and potentially develop a centrifugation method that involves centrifuging a sample in multiple orientations.

These studies examined the effects of centrifugation in removing marrow as a potential method of enhancing the bone incorporation of a graft. Marrow removal functions to both mitigate the risk of an immune response[5,6,11] and improve the osteoconduction of the graft so that host cells might be able to move in and remodel the bone. It is unclear how much marrow removal is needed to achieve these benefits and there is study indicating that some remaining marrow may aid in bone remodel.[2] Thus, future analysis could assess the controlled cleansing mechanisms to modulate the amount and pattern of marrow release and their effect on the efficacy of bone incorporation.

3.3 References

1. Bugbee WD, Pallante-Kichura AL, Görtz S, Amiel D, Sah R: Osteochondral allograft transplantation in cartilage repair: Graft storage paradigm, translational models, and clinical applications. *J Orthop Res* 34:31-8, 2016.

2. During A, Penel G, Hardouin P: Understanding the local actions of lipids in bone physiology. *Prog Lipid Res* 59:126-46, 2015.

3. Eagle MJ, Man J, Rooney P, Kearney JN: Comparison of bone marrow component removal from processed femoral head bone from living and deceased donors: presence of geodes in living donor bone can prevent maximum removal of marrow components. *Cell Tissue Bank* 19:727-32, 2018.

4. Eagle MJ, Man J, Rooney P, McQuillan TA, Galea G, Kearney JN: Assessment of a closed wash system developed for processing living donor femoral heads. *Cell Tissue Bank* 18:547-54, 2017.

5. Lewandrowski KU, Rebmann V, Päßler M, Schollmeier G, Ekkernkamp A, Grosse-Wilde H, Tomford WW: Immune response to perforated and partially demineralized bone allografts. *J Orthop Sci* 6:545–55, 2001.

6. Markel MD: Bone Grafts and Bone Substitutes. In: *Equine Fracture Repair,* ed. by AJ Nixon, Wiley-Blackwell, 2020, 163-72.

7. Meyer MA, McCarthy MA, Gitelis ME, Poland SG, Urita A, Chubinskaya S, Yanke AB, Cole BJ: Effectiveness of lavage techniques in removing immunogenic elements from osteochondral allografts. *Cartilage* 8:369-73, 2017.

8. Sherman SL, Garrity J, Bauer K, Cook J, Stannard J, Bugbee W: Fresh osteochondral allograft transplantation for the knee: current concepts. *J Am Acad Orthop Surg* 22:121-33, 2014.

9. Smith CA, Richardson SM, Eagle MJ, Rooney P, Board T, Hoyland JA: The use of a novel bone allograft wash process to generate a biocompatible, mechanically stable and osteoinductive biological scaffold for use in bone tissue engineering. *J Tissue Eng Regen Med* 9:595-604, 2015.

10. Sun Y, Jiang W, Cory E, Caffrey JP, Hsu FH, Chen AC, Wang J, Sah RL, Bugbee WD: Pulsed lavage cleaning of osteochondral grafts depends on lavage duration, flow intensity, and graft storage condition. *PLoS One* 12:e0176934, 2017.

11. VandeVord PJ, Nasser S, Wooley PH: Immunological responses to bone soluble proteins in recipients of bone allografts. *J Orthop Res* 23:1059-64, 2005.